Master of Science Thesis in Electrical and Mechanical Engineering
Department of Electrical Engineering, Linköping University, 2018

Optimal Platooning of Heavy-Duty Vehicles

Rikard Ohlsén and Erik Sten

LINKÖPING
UNIVERSITY

Master of Science Thesis in Electrical and Mechanical Engineering

Optimal Platooning of Heavy-Duty Vehicles

Rikard Ohlsén and Erik Sten

LiTH-ISY-EX–18/5119–SE

Supervisor: **PhD student Viktor Leek**
ISY, Linköping University
PhD student Olov Holmer
ISY, Linköping University

Examiner: **Professor Lars Eriksson**
ISY, Linköping University

Division of Vehicular Systems
Department of Electrical Engineering
Linköping University
SE-581 83 Linköping, Sweden

Sammanfattning

Fordons- och transportindustrin strävar ständigt efter att minska bränsleförbrukningen och för lastbilar finns det flera olika metoder. Två metoder som i tidigare arbete visat sig minska bränsleförbrukningen är look-ahead control (LAC) och kolonnkörning. LAC använder kunskap om framtida vägtopografi för att kunna optimera fordonets hastighet. Kolonnkörning är när lastbilar kör relativt nära varandra med syftet att minska luftmotståndet. Fordon i en kolonn kan även optimera sin hastighet baserat på framförvarande lastbil, vilket kallas adaptive look-ahead control (ALAC).

LAC/ALAC möjliggör användandet av pulse-and-glide (PnG) strategin, vilket innebär att ett fordon lägger i neutral växel och frirullar i t.ex. en nedförsbacke och därigenom minska sin bränsleförbrukning. Huvudsyftet med denna uppsats var att studera just hur fordon i en kolonn och kontrollstrategin känd som pulse-and-glide (PnG) interagerar när man eftersträvar lägre bränsleförbrukning. En fordonsmodell, en kolonnmodell och optimeringsbaserade regulatorer (LAC/ALAC) utvecklades. För de optimeringsbaserade regulatorerna valdes dynamisk programmering (DP) som optimeringslösare.

Resultaten visar att kombinationen av dessa metoder har stor potential och ger betydande bränslereduktion, både för enskilda fordon och för kolonnen som helhet. När det gäller bränsleförbrukning är den mest lämpliga strategin för kolonnen som helhet nära relaterad till den för enskilda fordon. De strategier som uppnådde högsta individuella bränslereduktion på fordonsnivå är också de som uppnådde högsta totala bränslereduktion för hela kolonnen. Enligt erhållna resultat bör det ledande fordonet utnyttja både LAC och PnG, medan de andra kolonnfordonen bör använda ALAC för att på så sätt också kunna nyttja PnG samtidigt som de upprätthåller ett kort avstånd till framförvarande fordon.

Resultaten visar att den största möjliga bränslereduktionen uppnås för downhill-segmentet och när alla metoder kombineras. För det sista fordonet i platongen är det så högt som 42%, jämfört med det nominella fallet (ett enda fordon som använder konventionell farthållare och inte växlar). Potentialen i bränslereduktion för segmentet platt och uppåt är likartat med varandra, 22% respektive 20%. Det är viktigt att påpeka att PnG i samtliga tre fall står för ungefär 1-3 procentenheter av hela bränsleduktionen. I verkligheten är vägtoppografi också ständigt varierande, så det är lovande att det finns en förbättring av bränsleeffektiviteten för alla typer av vägsegment.

Enligt resultaten erhålls största möjliga bränslereduktion vid en nedförsbacke. För det sista fordonet i konvojen är det så högt som 42 %, jämfört med det nominella fallet (ett fordon som använder konventionell farthållare och inte växlar). Den potentiella bränslereduktionen för plan väg och uppförsbacke är snarlika, 22 % respektive 20 %. För alla tre segmenten står PnG för cirka 1–3 procentenheter av hela konvojens bränslereduktion. I verkligheten är vägtopografin ständigt varierande, så det är även lovande att bränsleeffektiviteten förbättras för alla vägsegment.

Abstract

The vehicle and transport industry have a constant strive towards reduced fuel consumption and for HDVs are there numerous of different approaches. Two approaches that have been proven to reduce fuel consumption in previous work are look-ahead control (LAC) and platooning. LAC uses knowledge about the future road topography to optimize the vehicles velocity. Platooning is when HDVs drive relatively close to each other in order to reduce air drag. Platooning vehicles can also optimize their velocity based on the preceding vehicles trajectory, known as adaptive look-ahead control (ALAC).

Utilizing LAC/ALAC can enable a pulse-and-glide (PnG) strategy, where the vehicle engages neutral gear and freewheels e.g. in a downhill. Thereby reduces the fuel consumption. So, the main purpose of this thesis was to study how platooning vehicles and the control strategy known as pulse-and-glide (PnG) interact when pursuing lower fuel consumption. Therefore, a vehicle model, a platoon model and optimization-based controllers (LAC/ALAC) were designed and developed. For the optimization-based controllers was dynamic programming (DP) chosen as optimization solver.

The results shows that the combination of these approaches has a great potential to enable substantial fuel reduction, both for individual vehicles and for the entire platoon. The most suitable strategy, in terms of fuel consumption, for the platoon as a whole is closely related to the one for individual vehicles. The strategies resulting in the largest fuel reduction for a single vehicle does also give the largest total fuel reduction for the platoon as a whole. According to the results, a lead vehicle should utilize both LAC and PnG. The other platooning vehicles should employ ALAC in order to also utilize PnG meanwhile keeping a short intermediate distance.

According to the results the greatest potential fuel reduction is achieved for the downhill segment. For the last vehicle in the platoon it is as high as 42 %, compared to the nominal case (a single vehicle using conventional cruise control and not shifting gears). The potential fuel reduction for the flat and uphill segments are similar to each other, 22 % and 20 % respectively. For all three segments PnG accounts for roughly 1-3 percentage points of the entire platoons fuel reduction. In reality the road topography is constantly varying, so it is also promising that the fuel efficiency is improved for all types of road segments.

Acknowledgments

This thesis was supported by *Swedish Governmental Agency for Innovation Systems* under the program *Strategic Vehicle Research and Innovation*, grant FROST (2016-05380), Scania and Linköping University. We would like to thank the Vehicular Division at Linköping University and Lars Eriksson who gave us the opportunity to work with this thesis. We would also like to express a special thanks to our supervisors Viktor Leek and Olov Holmer for great support, inspiration and ideas.

Linköping, Juni 2018
Rikard Ohlsén och Erik Sten

Contents

Notation

Abbreviations

Abbreviation	Meaning
PnG	Pulse-and-glide
PID	Proportional, integral, derivative controller
ICE	Internal combustion engine
LAC	Look-ahead control
ALAC	Adaptive look-ahead control
DP	Dynamic Programming
EM	Electric motor
HDV	Heavy-duty vehicle
SQP	Sequential quadratic programming
ADAS	Advanced driver assistance systems
CC	Cruise control
ACC	Adaptive cruise control
EACC	Extended adaptive cruise control
V2V	Vehicle to vehicle
V2I	Vehicle to infrastructure
SFC	Specific fuel consumption
CTG	Constant time-gap
WL	Willans Line
EWL	Extended Willans Line
MVEM	Mean Value Engine Model

1 Introduction

Transportation done by road-vehicles is vital for the modern society and economy, goods that are produced or stored at a certain location often needs transport to get closer to the end consumer. The goods could be anything from groceries, building materials to fuel. In the European Union, almost 75% [25, pp. 101] of total inland freight transport is done by road. These road transports made by heavy-duty vehicles (HDVs), fueled with diesel, accounted for 30 % of the EU's total vehicular CO_2 emissions in 2015 [16]. Simultaneously, only 5 % of the vehicle fleet in Europe consisted of HDVs [16]. Moreover, in 2010 Scania declared that 30 % of costs related to an HDV was derived from fuel [1]. Therefore, it is of great interest from both an economic as well as an environmental perspective to make these transports as efficient as possible.

The vehicle and transport industry have a constant strive towards reduced fuel consumption and for HDVs there are numerous of different approaches. Topical and trending approaches within the industry are i.a.; look-ahead control (LAC) and platooning. LAC uses knowledge about the future road topography when controlling the vehicles longitudinal velocity in order to e.g. reduce the fuel consumption [12]. Utilizing LAC can enable the pulse-and-glide (PnG) strategy, where the vehicle engages neutral gear and freewheels e.g. in a downhill. Platooning is when HDVs drive relatively close to each other in a convoy with the aim to reduce air drag, thereby reducing fuel consumption [2].

As mentioned above, there are different ways to reduce fuel consumption. One approach is to increase the efficiency of the ICE and thereby reduce the specific fuel consumption (SFC). I.e., consume less fuel while maintaining the same amount of work output [8, pp. 75-76]. However, the common denominator for LAC and platooning is that these approaches are not employed to increase the efficiency of the ICE. Instead, the aim is to utilize the engine in a more efficient way. In this thesis the latter technologies are employed to achieve fuel reduction by controlling the HDVs intelligently and organizing them in platoon formations.

1.1 Motivation

According to the automotive industry [12, pp. 2], any technology for long-haulage vehicles that promise to save 0.5 % or more in fuel is worth exploring. As concluded and proven by Hellström [12] and Alam [2], LAC and platooning each have the potential to reduce fuel consumption well above 0.5%. Combining these two strategies and pulse-and-glide have the prospects of giving an increase in fuel-efficiency that at a minimum lives up to the industry's requirement. Nonetheless, it is reasonable that their efficiency would be greater when combined than individually.

1.2 Purpose

The main purpose of this thesis was to study how vehicle platoons and the control strategy pulse-and-glide, enabled through LAC, interact when pursuing lower fuel consumption. Therefore, it was required to develop a vehicle model, a platoon model, as well as design and implement optimization-based control strategies for single HDVs and platooning vehicles.

1.3 Expected Results

Contribution was to be made by answering the questions

- What is the most suitable strategy for the entire platoon versus individual vehicles?
- Should the vehicles in a platoon use pulse-and-glide, or is it more beneficial with a fixed distance in order to achieve satisfactory driving for the entire convoy?
- How is the fuel reduction affected by the choice of the engine model's sophistication degree when performing numerical optimization?

The answers to the questions would be concluded based on mainly fuel consumption measures.

1.4 Thesis Outline

The thesis is divided into seven chapters, Chapter 2 covers related research and work within the subject field of this thesis. Chapter 3 gives a detailed description of the models; engine, vehicle and platoon. In Chapter 4 the look-ahead control for a single HDV is derived, including i.a. the optimal control problem and a dynamic programming algorithm. Chapter 5 contains i.a. a description of the deployed look-ahead control strategy for platooning vehicles. Simulation results are presented in Chapter 6 and Chapter 7 contains a brief discussion, conclusions and suggestions for future work.

1.5 Method

First, related research were examined for inspiration, ideas and to build a steady knowledge foundation regarding state of the art solutions. Thereafter, the planned work path was as follows:

- Develop a simulation environment in SIMULINK for a single HDV using existing models
- Extend the single HDV model to a platoon model in SIMULINK
- Develop and implement a cruise controller and an adaptive cruise controller in SIMULINK
- Develop and implement a look-ahead controller for a single HDV in MATLAB and an interface to SIMULINK
- Develop and implement an optimization-based control algorithm for the platoon in MATLAB and an interface to SIMULINK
- Continuously execute simulations and analyze results

1.6 Delimitations

This thesis is a simulation study, i.e. no real-life experiments or validations will be carried out. Regarding the vehicle model to be used, the flexibility of the driveline components will not be considered, they will be assumed stiff.

Brakes will not be considered when solving optimal control problems since it is not optimal. The impact of traffic will also be disregarded.

Last, the aim of this thesis is not to develop software feasible for on-board usage in a real environment. I.e., computational requirements and complexity will not be considered.

2

Related research

Related research within the subject field of this thesis is focused on three main areas; modeling, LAC and platoon control strategies.

2.1 Modeling

Modeling and simulation is important in the automotive industry due to the constantly increasing restrictions and harder emission regulations. Adding more than 120 years of continuously development of combustion engines makes it hard to easily attain significant improvements. A lot of research and development has already been done and implemented according to Ekberg et al. [7, pp. 1]. One way to meet the tougher regulations and increase efficiency is to use modeling and simulation. It is an efficient way to evaluate different solutions.

2.1.1 Engine

An engine model has been developed in Ekberg et al. [7]. It is a validated four state model with three actuator signals of a heavy-duty diesel engine and is stated to be suitable for simulation and optimization studies. The model is continuously differentiable and the four states are intake manifold pressure, exhaust manifold pressure, pressure after the compressor and turbocharger speed. The actuator signals are fuel injection per cycle, throttle position and wastegate position. It is divided into four sub-models; engine torque, cylinder air charge, engine stoichiometry and exhaust temperature.

In Alam [2], the author studied the effects of platooning and states in his future outlook that *"a more sophisticated engine model might possibly be required [...]"* [2, pp. 166]. The model produced in Ekberg et al. [7] is considered to satisfy this. Hellström [12] has conducted a detailed study of LAC for HDVs in which the author employs an engine model that also is considered less sophisticated than the one developed by Ekberg et al. [7].

For further reading on state-of-the-art engine modeling, the reader is referred to Eriksson and Nielsen [8].

2.1.2 Heavy-Duty Vehicle (HDV)

A longitudinal vehicle model for an HDV has been developed in Myklebust and Eriksson [24]. It has been validated against measurement data and was concluded to agreed well in simulations, both for high and low gears.

The modules that the model contains and information exchange between them are illustrated in Figure 2.1. Each module belongs to a part of the powertrain, which consist of ICE, clutch, gearbox, propeller shaft, final drive, drive shafts and vehicle dynamics. The ICE module is replaced with the model described in section 2.1.1.

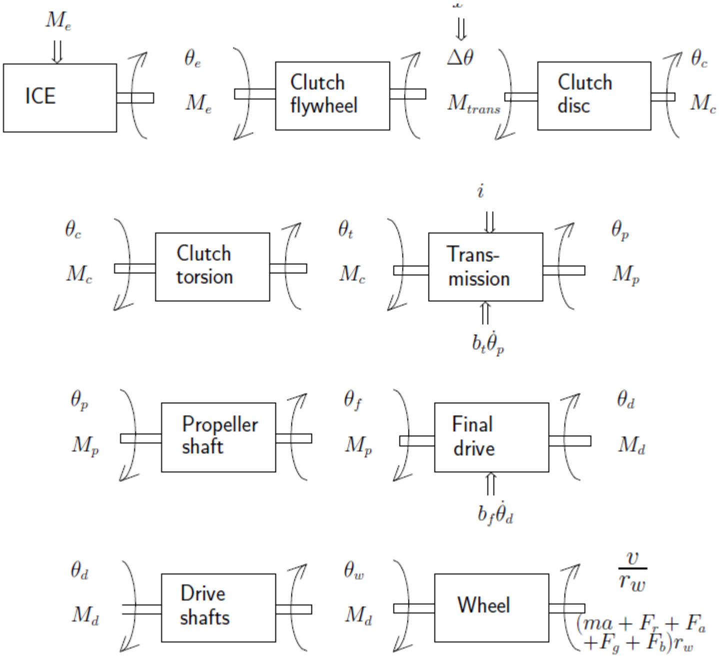

Figure 2.1: *A sketch of subsystems that are used in the vehicle model as well as the information exchange in between them, from Myklebust and Eriksson [24, pp. 2] with permission*

2.1.3 Platooning

The longitudinal platooning model proposed in Alam [2, pp. 95-97] is closely related to the single vehicle model proposed in the same thesis. The major difference between the singular vehicle model and platoon model is the scaling of aerodynamic drag based on inter-vehicle spacing. The scaling of air drag is caused by the preceding vehicle and is determined through empirical measurements.

To be able to capture the platoon dynamics, the longitudinal model is extended. By discretizing and introducing states that defines the inter-vehicle distance and control signal for maintaining the distance (basically throttle and break) it is possible to formulate the problem as a quadratic cost function.

Alam [2] qualitatively evaluates the model and control through experiments and it is stated that the results differ from simulations to some extent. However, simulations still mimics most of the dynamics that is seen in reality.

2.2 Look-Ahead Control (LAC)

A Look-Ahead controller uses knowledge about the HDVs position and future road topography when controlling the vehicles driving strategy. An optimal velocity trajectory is determined for the vehicle and its given route in order to lower fuel consumption. In the article by Hellström et al. [13], the author studies if the use of a look-ahead control for a single HDV can minimize the fuel consumption without increasing travel time. Using a road slope database and a GPS unit to determine current position and future topography, Hellström et al. designs a predictive control structure that uses Dynamic Programming (DP) to solve the optimization problem. The algorithm is constantly feeding the lower level controllers with new set points. It is a function of current position, velocity and gear. The same approach is also used in Alam [2]. The look-ahead control developed by Hellström et al. [13] was evaluated and achieved roughly a 3.5 % lower fuel consumption compared to solely cruise control [13]. Through computer simulations Lattemann et al. [19] and Terwen et al. [30] also proves the fuel saving potential of predictive cruise control. Both Lattemann et al. and Terwen et al. adds quadratic penalties on deviations from cruise speed. While, Hellström [12], Huang et al. [15] and Passenberg et al. [26] all considers a fuel-optimal control and includes time in the objective when minimizing the energy required for a mission.

2.2.1 Appropriate Optimization Solvers

Hellström et al. [13] and Alam [2] uses a DP algorithm to solve the optimal control problem. In comparison, Terwen et al. [30] employs a tailored direct multiple shooting algorithm, Huang et al. [15] a sequential quadratic programming (SQP) algorithm and Passenberg et al. [26] solves their multi-point boundary-value problem with an indirect multiple shooting algorithm. Broadly speaking, there are three general approaches to solving an optimal control problem [6]; Dynamic Programming, Indirect Methods; Direct Methods.

- Dynamic Programming (DP) [4] is an optimization method used to solving complex problems by dividing it into sub-problems. However, the method is limited to low dimensions, sustained from the phenomenon known as

Bellman's "curse of dimensionality" [5]. The phenomenon describes the problem caused by discretization of the continuous variables as it leads to exponential increase in complexity.

- Indirect Methods [6] can simply be outlined as; first optimize, then discretize. First, the approach analytically constructs the necessary conditions for optimality of the infinite dimension problem. From that a boundary value problem is derived which is solved numerically. However, it can be difficult to solve differential equations due to nonlinearities and instability as well as higher index differential-algebraic equations can arise.

- Direct Methods, compared to Indirect Methods, discretizes the original infinite optimization problem directly and then converts it into a finite dimensional nonlinear programming problem [6]. Thereafter the nonlinear programming problem is solved using numerical optimization methods such as, e.g., sequential quadratic programming.

The dimension of state space is low in the work done by Hellström [12] which enables the use of DP to find the optimal control law for the switching nonlinear mixed-integer problem. Moreover, Hellström [12] argues that as a quite long horizon is to be used it is favourable to use DP as its computational complexity is linear.

2.2.2 Algorithm Design

In a closer perspective Hellström et al. [14] developed a DP algorithm for fuel-optimal control with low computational effort and thereby enabling efficient on-board LAC for HDVs. Proper inclusion of gear shifting was given to achieve optimal velocity profile and gear selection, i.a. lower fuel consumption. The aim was computational efficiency, so the algorithms complexity and numerical errors were analyzed. Hellström et al. shows that to avoid oscillating solutions and cut back interpolation errors, it is favourable to formulate the problem in terms of kinetic energy instead of velocity.

2.2.3 Pulse-and-Glide (PnG)

The case study by Walnum and Simonsen [33] shows that driving behaviours does affect the fuel consumption and HDVs should, when possible, utilize rolling without engine load to lower the fuel consumption. I.e., employ the pulse-and-glide strategy where the HDV is driving in neutral gear (running idle) during e.g. a down hill and thereby allowing fuel savings.

Through simulations, Turri et al. [32] studies, i.a., the effects of exploiting freewheeling when employing fuel-optimal LAC and a DP algorithm to solve the optimal control problem. The variation of running idle and propulsion at the optimal torque enables more efficient usage of the engine. Results presented by Turri et al. shows that the HDV who exhibits PnG behavior can save up to

4% in fuel consumption compared to driving without the possibility to exploit freewheeling.

Moreover, In McDonough et al. [21] and McDonough [22] the authors studies time-varying vehicle speed oscillations for cars in traffic environments. Their time-varying speed profiles resembles the PnG strategies that has been mentioned in previous work and proven to be more fuel efficient than driving with a constant velocity. In both cases, the authors have demonstrated improvements in fuel consumption by more than 4 %. McDonough et al. [21] used a virtual testing environment based on CarSim while McDonough [22] executed actual vehicle experiments.

2.3 Platoon Control Strategies

Platooning is when HDVs are positioned relatively close behind each other in order to reduce air drag. Reducing the energy required to accelerate or maintain speed, compared to not having a preceding HDV. By utilizing platooning in a structured and controlled manner there is a substantial potential for reduced fuel consumption. In Alam [2], the author identifies the fuel saving potential when utilizing platooning to be 4.7-7.7 %. Depending on configurations such as distance between the HDVs and number of HDVs in the platoon.

The implementation of more sensors and control systems to vehicles have enabled more advanced functionality and features. A section of the new features that have been developed are the advanced driver assistance systems (ADAS). Under this section falls e.g. adaptive cruise control (ACC) and safety systems such as lane departure warnings that alerts the driver when leaving the current lane unintentionally.

To achieve efficient HDV platooning there have to be automated systems that takes care of the control. Alam [2] studies the concept of platooning and related strategies such as automated control and vehicle to vehicle (V2V) communication. The increase of more advanced hardware in the HDVs is an enabler for the development of commercially applicable platooning technologies. Key technologies such as V2V and vehicle to infrastructure (V2I) communication have now matured and is possible to use in real world applications [2, pp. 7-8].

2.3.1 Platoon without V2V Communication

ACC can be seen as an extension to a regular cruise controller (CC). While a conventional CC tries to maintain a fixed speed at all times, the ACC tries to maintain a fixed speed unless there is a vehicle in front. If there is a preceding vehicle, the ACC adapts its current speed to the preceding vehicle and maintains a distance dependent on the speed instead (a constant time gap, see Section 5.1). Hence, there is no V2V communication needed for the basic ACC technology. Moreover, the technology enables an elementary form of platooning and makes it easy for the driver to keep a certain distance. However, by not knowing how the preceding vehicle will act, safety is reduced and non-optimal braking and acceleration events might occur. For a more comprehensive description of ACC, refer to Axehill and Sjöberg [3] and Rajamani [28].

An extension to this strategy could be to implement LAC (described in section 2.2) for the lead vehicle and using ACC for the following vehicle. The idea is to make the platooning more efficient by making the lead trucks velocity trajectory propagate down to the following vehicle. In the master thesis by Ling and Lindsten [20], the authors studies this strategy by employing neural networks in combination with ACC to predict the lead vehicles velocity trajectory without communication. However, Ling and Lindsten conclude that using LAC individually for each HDV sometimes outweigh the benefits of operating in a platoon.

2.3.2 Platoon with V2V and V2I Communication

To increase the efficiency of platooning the HDVs could communicate with each other. An approach supported by Alam, he states: *"The individual optimal LAC strategies are not consistent with maintaining a constant inter-vehicle spacing for air drag reduction, which is the aim in HDV platooning."*[2, pp. 119]. However, platooning with V2V and/or V2I communication can be divided into two general fields, cooperative and non-cooperative. Here, cooperative implies that an overall approach is employed for the whole platoon and the vehicles are willing to change their individual velocity strategies in order to serve the common goal.

Non-Cooperative Look-Ahead Control

An approach that makes use of V2V communication but does not utilize an overall strategy for the whole platoon (lead vehicle is not willing to change its optimal velocity strategy) is presented in Turri et al. [32]. I.e. non-cooperative platooning. The idea is to feed the velocity trajectory of the preceding HDV (constructed by LAC) to the following HDV. Based on the lead HDV's trajectory, the following HDV then optimizes its own driving mission. Turri et al. evaluated the non-cooperative approach together with elements mentioned earlier; LAC, DP, ACC and PnG. Noteworthy is that the author has used an inter-vehicle distance reference as a state in his DP algorithm. The presented simulation results show a fuel saving potential for the following HDV by as much as 18 %. However, Turri et al. only investigated this approach for a two vehicle convoy where solely the following vehicle is allowed to PnG when platooning occurs.

Alam [2] studies how the same approach can be utilized for larger platoons and refers to it as Adaptive Look-Ahead Control (ALAC). The author's developed control architecture consist of decentralized adaptive LAC (ALAC), where the planned velocity profile of the preceding vehicle is received through V2V communication. Thereafter, the velocity profile is adaptively optimized along with the added constraint of keeping the distance to preceding vehicle. Alam also uses DP to solve the optimal control problem but does not have inter-vehicle distance as a state. Last, it should be mentioned that the control strategy employed by Ling and Lindsten [20] could be referred to as ALAC.

Cooperative Look-Ahead Control (CLAC)

When employing CLAC, both Alam [2] and Turri et al. [31, pp. 5-6] propose a two layer control architecture that make use of V2V communication and optimizes for the platoon as a whole, cooperative platooning.

The bottom layer consist of individual decentralized vehicle controllers that are equipped with V2V communication technology which enables broadcasting of relevant information. The top layer is a centralized platoon coordinator that communicates with each vehicle (V2I) and suggests a common strategy. The velocity trajectory is based on information about i.a. road topography and individual vehicle parameters. It considers the constraints of the individual vehicles which guarantees that every vehicle in the platoon will be able to track the suggested velocity trajectory. The average speed constraint is also taken into consideration, that is set to manage a certain distance in a limited time frame. This trajectory is fed down to each HDV from the coordinator and the bottom layer controller's mission is to track and minimize the deviation from the suggested overall velocity trajectory. Since all the safety-critical features are in the bottom layer controller and the top layer is not related to a specific vehicle it can be based off-board (infrastructure) or in any of the HDVs.

Both Alam [2] and Turri et al. [31] prove that a fuel reduction is achieved due to the employment of CLAC. However, even though the overall architecture is basically the same in Alam [2] and Turri et al. [31], there are some differences. Alam, the top layer receives an individual LAC strategy for each vehicle in the platoon and thereafter derives a function that yields a maximum variation for a specific LAC velocity profile. I.e., the CLAC algorithm considers all LAC velocity profiles and then chooses the one requiring largest modifications to be the common profile for all vehicles.

Turri et al. [31] on the other hand, employs a LAC in the top layer that exploits topography information and constraints for each vehicle when computing the platoon's fuel-optimal velocity profile. Here, Turri et al. uses a non-linear model and a DP algorithm to solve the optimal control problem. Regarding the bottom layer, the author suggests a Model Predictive Controller (MPC) in each vehicle which tracks the velocity profile and desired distance to preceding vehicle transmitted from the top layer. Moreover, the MPC uses a linear model in it computations and a quadratic programming approach to solve the optimal control problem.

3

Modeling

This chapter first presents the developed model for a single HDV and a platoon model.

3.1 Vehicle Model

In this section, the dynamic model for a single HDV will be described, the subsections are Longitudinal Model, Powertrain Model, Engine Models, Driveline, Gear Shift Model and Vehicle Freewheeling Model.

3.1.1 Longitudinal Model

A model was formulated for the longitudinal dynamics when the HDV is considered to move in one dimension, see Figure 3.1. Forces acting on the vehicle in motion are presented in Table 3.1 and explanations of the model parameters are found in Table 3.2. The states are velocity v, current gear g, and the vehicles distance s. Control signals are fueling u_f, gear u_g, and brake u_b.

Table 3.1: *Longitudinal Forces*

Variable	Description	Expression
$F_a(v)$	Air drag force	$\frac{1}{2} c_D A_a \rho_a v^2$
$F_r(s)$	Rolling resistance	$m g_0 c_r cos\alpha(s)$
$F_g(s)$	Gravitational force	$m g_0 sin\alpha(s)$
$F_b(u_b)$	Force produced by brakes	$m g_0 \mu u_b$, if $v > 0$
$F_p(v, g, u_f)$	Propulsive force	see Section 3.1.2

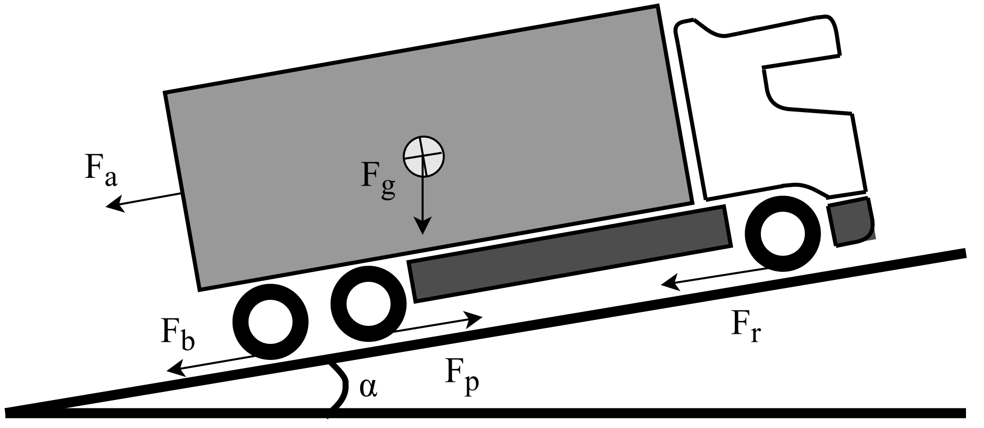

Figure 3.1: *Illustration of the forces acting on a vehicle when considered moving in one dimension*

Table 3.2: *Parameters - Longitudinal Forces*

Symbol	Description	Unit
c_D	Air drag coefficient	[-]
ρ_a	Air density	[kg/m^3]
m	Vehicle mass	[kg]
α	Road slope	[degrees]
A_a	HDV cross section area	[m^2]
μ	Traction coefficient	[-]
g_0	Gravity constant	[m/s^2]
c_r	Rolling resistance coefficient	[-]

By using Newton's second law of motion the longitudinal model can be defined as

$$F_p - F_a - F_r - F_g - F_b = m\frac{dv}{dt} \tag{3.1}$$

However, as the road slope depends on position, it is reformulated using spatial coordinates

$$F_p(v, g, u_f) - F_d(s, v, u_b) = mv\frac{dv}{ds} \tag{3.2}$$

Where $F_d = F_a + F_r + F_g + F_b$. The propulsive force is generated from torque in the engine that propagates down in the driveline and translates to force. The reason to why F_p has velocity and gear as states is that the engine speed ω_e is based on vehicle speed and current gear. It will be explained further in section 3.1.2.

Kinetic Energy Formulation

Kinetic energy is defined as

$$e = \frac{1}{2}mv^2 \tag{3.3}$$

and in combination with the relations

$$\frac{dv}{dt} = v\frac{dv}{ds} = \frac{1}{2}\frac{d}{ds}v^2 \tag{3.4}$$

it enables reformulation of the model (3.2) in terms of kinetic energy

$$mv\frac{dv}{ds} = \frac{m}{2}\frac{d}{ds}v^2 = \frac{de}{ds} = F_p - F_d\left(s, \sqrt{\frac{2e}{m}}\right) \tag{3.5}$$

Formulation in terms of kinetic energy is utilized as it reduces the risk of oscillating solutions and linear interpolation errors when performing numerical optimization [12].

3.1.2 Powertrain Model

The powertrain model used in the vehicle model consists of the following components; engine, clutch, transmission, propeller shaft, final drive, drive shafts and wheels. See Figure 3.2. In simulations the engine is a separate model that is called upon from the vehicle model that consists of the driveline and forces acting on the HDV.

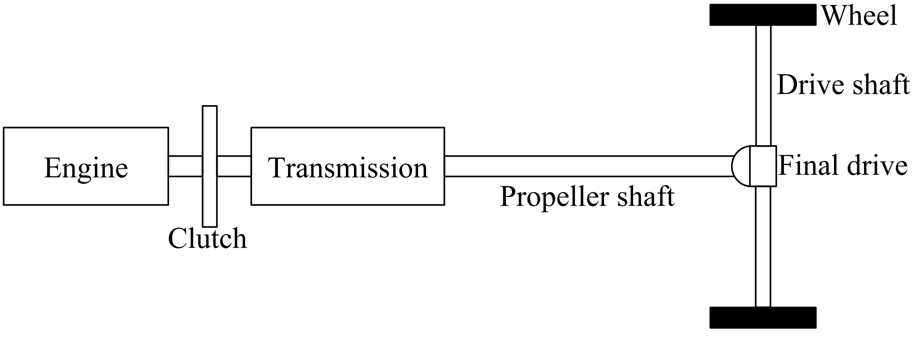

Figure 3.2: *A sketch of the vehicles powertrain*

3.1.3 Engine Models

Three different approaches to engine modelling will be outlined in this Subsection. All representing different degrees of complexity and sophistication.

The least complex models were the ones utilized when executing numerical optimization. It was desired to study the impact of deploying engine models of different complexity when retrieving the fuel consumption through simulations. Hence, the multiple engine models.

Willans Line Approximation

First, a simple but yet useful engine model [11], the Willans Line Approximation. A Willans Line model consist of an affine representation and makes use of the concept where input energy is converted into output work and external losses [29]. I.e., the engine model will output engine torque (M_e) based on fueling (u_f), an energy converter (W_e) and a constant external loss (W_{loss}).

$$M_e(u_f) = W_e u_f - W_{loss}$$

Extended Willans Line Approximation

The Extended Willians Line Approximation is based on the same principle as the simpler WL Approximation just described. However, for the EWL model, both the energy converter and external loss depend on the engine's rotational speed (ω_e).

$$M_e(u_f, \omega_e) = W_e(\omega_e)u_f - W_{loss}(\omega_e)$$

Complete Mean Value Engine Model

Last, the most complex and sophisticated engine model, adopted from Ekberg et al. [7]. It consists of validated sub-models that captures the dynamics of the engine. In order to be suitable for simulation and achieve a low computational time the number of states are limited to four, $x_{ice} = [p_{caf}\ p_{im}\ p_{em}\ \omega_t]$. The dynamics of these states are described in the engine model and utilized when simulating. The engine's controller inputs are $u_{ice} = [u_f\ u_{thr}\ u_{wg}]$. See Table 3.3 for descriptions of the states and control signals. Moreover, the engine model has one exogenous input, the engine speed ω_e. The dynamics of the engine speed are described in the vehicle model, based on vehicle speed and current gear, see Equation (3.13). This engine speed is then used within the engine model. See Figure 3.3 for an illustration of states, control signals and communication between models.

Since the aim of this thesis is not to capture specific dynamics of the engine in terms of throttle and wastegate control, they will be kept constantly open and closed respectively. In practice this means that only one control signal will be varying, the fueling of the engine u_f. The engine model will output engine torque (M_e) based on fueling and engine speed, which then propagates down through the driveline and translates to propulsive force.

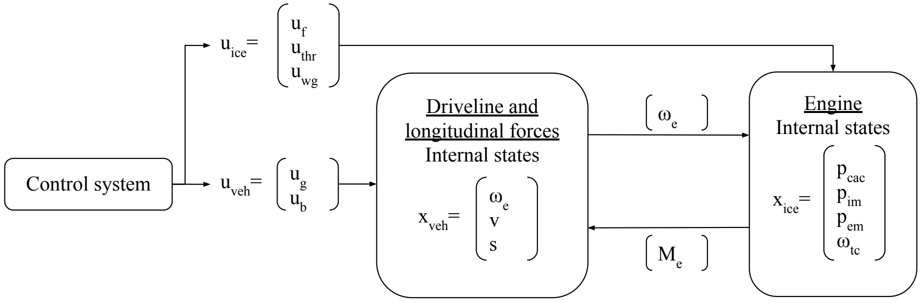

Figure 3.3: *An overview of the states and control signals for the MVEM and communication between the models*

Table 3.3: *States and control signals - Engine*

Type	Symbol	Description	Unit
State	p_{caf}	Pressure after compressor	[Pa]
State	p_{im}	Pressure in intake manifold	[Pa]
State	p_{em}	Pressure in exhaust manifold	[Pa]
State	ω_t	Turbocharger rotational speed	[rad/s]
Control signal	u_f	Injected fuel	[mg/cycle]
Control signal	u_{thr}	Throttle position	-, [0-1]
Control signal	u_{wg}	Wastegate position	-, [0-1]

Fuel Consumption

The fuel consumption can be obtained through the fuel mass flow, given as

$$\dot{m} = \frac{n_{cyl}}{2\pi n_r}\omega_e u_f = \frac{n_{cyl}}{2\pi n_r}\frac{i}{r_w} v u_f \tag{3.6}$$

where the parameters are explained in Table 3.4.

3.1.4 Driveline

The driveline makes up all the components of the powertrain except for the engine. It is modeled as stiff, which implies that no torsion is considered in the driveline components. Moreover, the components are also assumed ideal, meaning that no losses occur between them. Utilizing these assumptions, one can easily derive the relationship between vehicle speed and engine torque to engine speed and propulsive force. The variables used are summarized in Table 3.4 together with parameters related to the powertrain and engine.

Since the engine speed is derived from vehicle velocity and current gear it is natural to start with a given velocity and trace the speeds backwards in the driveline. The propulsive force however, is a result of engine torque and current gear. Therefore, it is natural to start with a given engine torque and trace the torque down in the driveline to a resulting propulsive force. Based on this, the structure below starts with vehicle velocity and ends with propulsive force. It is assumed that the clutch has no slip and is engaged at all times.

Table 3.4: *Parameters and variables - Powertrain*

Symbol	**Description**	**Unit**
M_e	Net torque produced by engine	[Nm]
M_{tr}	Torque from transmission	[Nm]
M_f	Torque from final drive	[Nm]
M_w	Torque on wheels	[Nm]
i_{gear}	Gear ratio in transmission	[-]
i_{final}	Final drive gear ratio	[-]
i_{tot}	Total ratio ($i_{gear}i_{final}$)	[-]
r_w	Wheel radius	[m]
ω_e	Engine rotational speed	[rad/s]
ω_{tr}	Transmission output rotational speed	[rad/s]
ω_d	Driveshaft rotational speed	[rad/s]
ω_w	Wheel rotational speed	[rad/s]
v	Vehicle speed	[m/s]
$\dot{m}$	Fuel mass flow	[m^3/s]
n_{cyl}	Number of cylinders	[−]
n_r	Revolutions per stroke	[−]

Under the assumption that there is no wheel slip the the relation between wheel rotational speed and velocity of the vehicle is given by

$$\omega_w = \frac{v}{r_w} \tag{3.7}$$

Drive shaft rotational speed is the same as wheel rotational speed that together with the final drive gear ratio gives the propeller shaft rotational speed (transmission output rotational speed)

$$\omega_{tr} = \omega_d i_{final} = \omega_w i_{final} \tag{3.8}$$

By knowing the current gear ratio, i.e. current gear in the transmission, the engine speed is given by following equation

$$\omega_e = \omega_{tr} i_{gear} \tag{3.9}$$

Now when current engine speed is given, it is possible to calculate the torque outputted by the engine. The resulting net torque is transferred through the transmission and into the propeller shaft, with the following relation

$$M_{tr} = i_{gear} M_e \tag{3.10}$$

Transfer of torque from the stiff propeller shaft to the drives shaft is transferred through the final drive, that has a fixed gear ratio. Since the drive shafts are stiff, the transfer of torque applies directly to the wheels. Resulting in following equation

$$M_f = M_w = i_{final} M_{tr} \tag{3.11}$$

Under the assumption that there is no wheel slip, the following relation is given for the vehicle propulsive force.

$$F_p = \frac{M_f}{r_w} \tag{3.12}$$

Equations (3.7) - (3.12) gives the following relations.

$$\omega_e = \frac{v}{r_w} i_{tot} \tag{3.13}$$

$$F_p = M_e \frac{i_{tot}}{r_w} \tag{3.14}$$

3.1.5 Gear Shift Model

During a gear shift event several parts of the engine and driveline are affected. The fundamental idea with a gear shift is that the engine is able to output a different rotational speed which corresponds to the same vehicle speed as before the shift thanks to a different transmission ratio. A lower engine speed is required if an up-shift occurs and vice-versa if a down-shift occurs. However, the engine is not able to change speed instantly and the transmission is not able to change gear instantly either. Therefore, the vehicle will lose the propulsive force generated by engine torque while a gear shift occurs.

The approach taken when modeling a gear shift is a simplified version of *"gear shifting by engine control"* presented in Pettersson and Nielsen [27]. The basic idea is to reduce the produced net engine torque to zero, engage neutral gear, synchronize the engine speed to the new speed required after completed gear shift, engage the new gear and finally increase the net engine torque. The propulsive force will be zero when in neutral gear, as i_{gear} will be zero. Studying Equation (3.14) this becomes obvious. When reducing the net engine torque to zero the fuel injection is reduced significantly since the only fuel needed is to overcome the torque required to rotate the engine, i.e. overcome e.g. internal friction.

In Pettersson and Nielsen [27] it is stated that there is a need for a so called *"torque control phase"*, which refers to the need to ramp down the torque produced by the engine before engaging neutral gear. This is needed due to the driveline oscillations otherwise produced. However, since the modeled driveline is stiff and the gear shifting is simplified, this is not taken into account.

To illustrate how the sequence is modeled and performed, a typical gear shifting event is presented in Figure 3.4. It is a gear shift from gear 11 to gear 12. As can be seen in the top plot, the sequence begins with the reference gear indicating a new desired gear. By knowing the desired gear to shift to, it is possible to predict the required engine speed (based on velocity). This can be seen in the second plot. When engaging neutral gear (start of actual gear shift), the propulsive force is instantly lost. The fuel injection is reduced and the engine torque becomes very close to zero. During the gear shift the engine speed synchronize with the new engine speed desired. When the synchronization is completed the correct gear is engaged together with increased fuel injection, net engine torque and propulsive force.

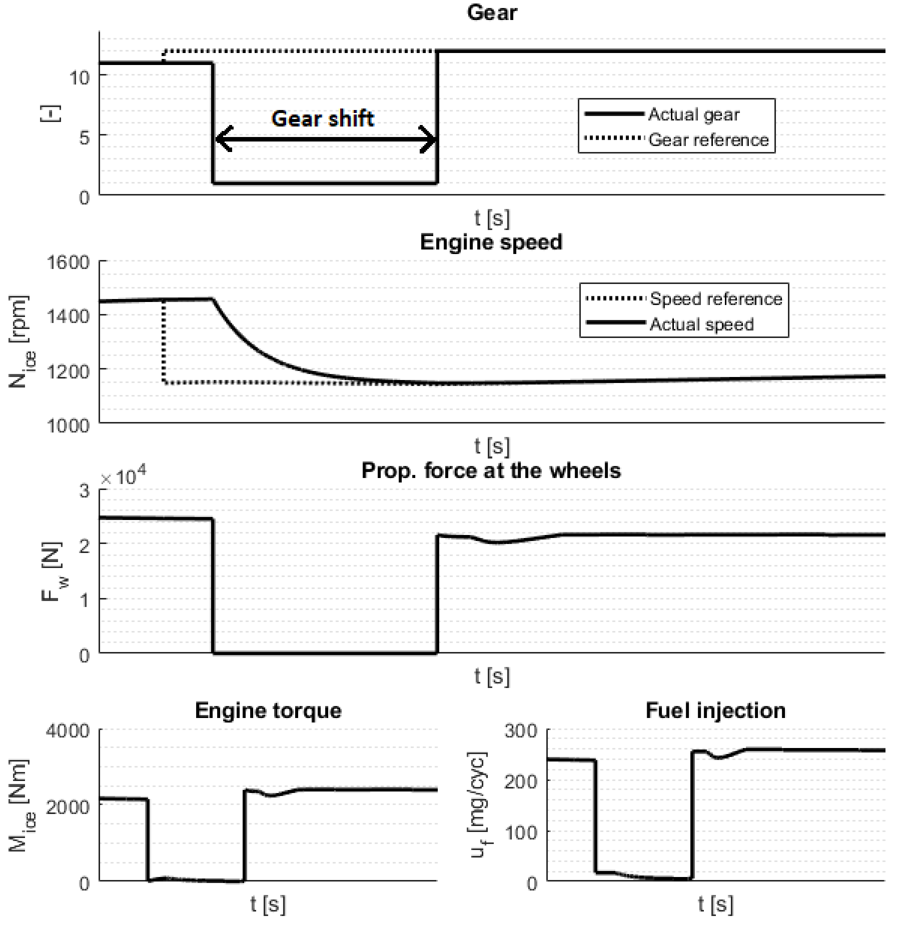

Figure 3.4: Gear shift sequence for a shift from gear 11 to 12. Illustrating how the engine and driveline is affected by a gear shift.

3.1.6 Vehicle Freewheeling model

To be able to utilize the pulse-and-glide strategy there is a need for the vehicle to be able to engage neutral gear and stay in that gear until a new gear is demanded. The basics of the gear shift sequence presented above is still used. Indicating that the propulsive force will be zero and the forces acting on the vehicle will solely be the resistive forces. However, when engaging freewheeling the reference gear is neutral gear and the desired engine speed is a predefined *idle speed*. Preferably set as low as possible to keep required fuel injection at a minimum.

3.2 Platoon Model

The air drag force acting on a vehicle was earlier defined as

$$F_a(v) = \frac{1}{2} c_D A_a \rho_a v^2 \tag{3.15}$$

However, in a platoon of HDVs, the vehicles' air drag coefficient, c_D, depends on the distance between preceding and following vehicle as well as position within the platoon. The air drag coefficient is generated by the relation $c_D = c_d(1 - f_i(d)/100)$ which scales the air drag coefficient c_d using a non-linear function f_i. Here, the approach taken was to employ a linearization of the non-linear function, more specifically, the linearization presented in Kemppainen [18].

$$f_1(d) = -0.9379d + 12.8966, 0 \leq d \leq 15 \tag{3.16a}$$

$$f_2(d) = -0.4502d + 43.0046, 0 \leq d \leq 80 \tag{3.16b}$$

$$f_3(d) = -0.4735d + 51.5027, 0 \leq d \leq 80 \tag{3.16c}$$

$$f_i(d) = f_3(d), i \geq 4 \tag{3.16d}$$

Figure 3.5, which the functions are derived from, illustrates how much the air drag coefficient is reduced due to position in the platoon and intermediate distance.

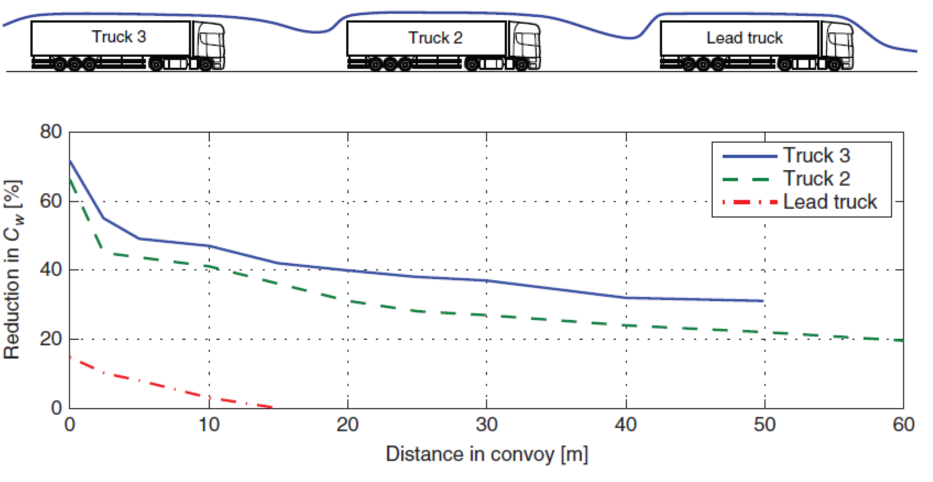

Figure 3.5: *Illustration of decreasing air drag coefficient for three vehicles in a platoon, from Eriksson and Nielsen [8] with permission*

4

Speed Control for Single HDV

First, this chapter will describe a traditional Cruise Controller (CC). Thereafter, introduce the optimal control problem and then outline the Look-Ahead Control (LAC). The control system architecture when utilizing LAC is such that the LAC feeds a velocity profile and desired gear down to lower level control, the CC.

4.1 Cruise Control (CC)

Traditionally a CC's objective is to track a given constant speed reference that is given by the driver. When a specific speed is set, the vehicle's systems automatically controls the throttle to obtain and maintain the desired speed. Since the developed LAC generates a speed reference, a conventional CC was developed which enables the vehicle to track the desired velocity trajectory.

The control strategy used for the CC was adopted from Rajamani [28] where a two level architecture is suggested. The control error between speed reference and current speed acts as input to the upper level controller and desired acceleration as output.

For the upper level controller a PI controller was used which is presented in equation (4.1).

$$\ddot{s}_{des}(t) = -k_p(V - V_{ref}) - k_I \int_0^t (V - V_{ref})dt \tag{4.1}$$

Where $\ddot{s}_{des}$ represents desired acceleration, V current speed and V_{ref} desired speed.

Due to limitations of the control signal and the above proposed controller there is a risk for integration windup. To avoid this, an anti-windup control was implemented.

The suggested lower level controller then takes desired acceleration as input and outputs desired throttle angle. However, the model described in chapter 3 is controlled directly on fuel injection and has a throttle that is constantly open. Therefore, a different approach is taken for the lower level controller, compared to the one suggested by Rajamani [28]. The demanded torque is needed to calculate required fuel. By utilizing information from the model it is possible to translate desired acceleration into desired net torque, see Equations (4.2) - (4.4).

$$i_{tot} = i_{gear} i_{final} \tag{4.2}$$

$$F_p = \ddot{s}_{des} m_{truck} + F_d \tag{4.3}$$

$$M_{des} = F_p \frac{r_w}{i_{tot}} \tag{4.4}$$

Where the parameters are explained in Tables 3.4 and 3.2. Once the desired engine torque is obtained, a proportional scaling was used to translate torque to u_f. By utilizing information from the model in a way that is described above as well as controlling fuel injection directly, a feasible CC was achieved.

If the HDV would exceed the reference velocity with a user specified velocity (V_{exc}) the breaks will be activated and break proportionally to the exceeded velocity with a chosen gain $K_{b,CC}$. Otherwise the braking force will be zero. This could also be used if the vehicle is not allowed to exceed a speed limit due to legal reasons ($V_{allowed}$), see Equation (4.5).

$$F_b = \begin{cases} 0, & \text{if } V - V_{ref} - V_{exc} \leq 0 \\ m g_0 \mu u_b (V - V_{allowed}) K_{b,CC}, & \text{if } V - V_{allowed} > 0 \\ m g_0 \mu u_b ((V - V_{ref}) - V_{exc}) K_{b,CC}, & \text{otherwise} \end{cases} \tag{4.5}$$

4.1.1 Verification of CC

When the CC was implemented in SIMULINK it was necessary to verify that it performs as expected. To do so there was a need for a test design and road profile that challenged the CC to handle variations in demanded velocity and road slope. The orchestrated drive mission presented in Figure 4.1 includes precisely these challenges. The verification is executed without any limitations on how much the vehicle is allowed to deviate from the reference speed. Which is the reason why the breaks never became active.

Initially, the vehicle drives on a flat road and the CC is set at 70 km/h, the CC then receives a step in demanded velocity to 80 km/h. Which it handles without any significant overshoot or other unwanted behaviour.

Thereafter, the CC handles three variations in slope; 1%, 1.5% and -1%. Also managed without any significant change in velocity.

Finally, the CC receives a negative step in demanded velocity, causing the vehicle to decelerate until the demanded velocity of 70 km/h is reached. No unwanted characteristics occurs.

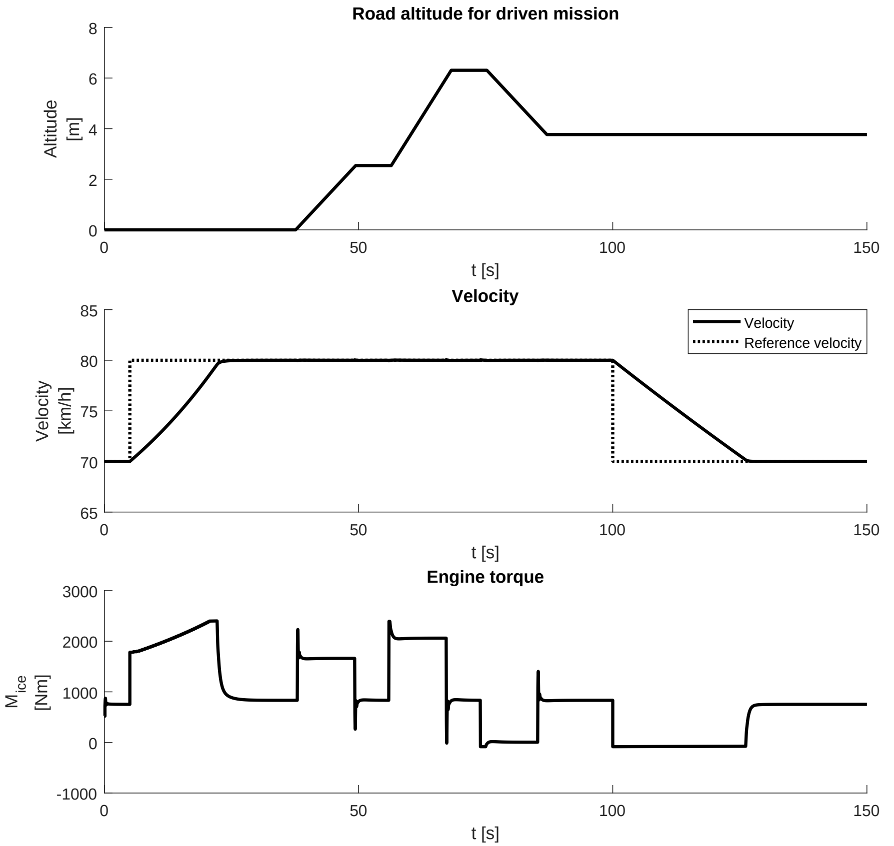

Figure 4.1: Verification of CC, including one positive step in velocity, three different road slopes and one negative step in velocity.

4.2 Optimal Speed Planning

The objective for a given mission is to minimize the consumed fuel M_{fuel} and complete the mission within a given time T_{max}. The optimal control problem (OCP) can be stated as

$$\begin{aligned} \text{minimize} \quad & M_{fuel} \\ \text{subject to} \quad & T \leq T_{max} \end{aligned}$$

However, the OCP can be reformulated to avoid the necessity of introducing time as a state and thereby desisting from the *Curse of Dimensionality* [5]

$$\text{minimize} \quad M_{fuel} + \beta T \tag{4.6}$$

Which is an approach used in Monastyrsky and Golownykh [23]. Here β represents a weight functionality, a trade-off between consumed fuel and mission time. It will be further elaborated in Subsection 4.2.1. The proposed cost function is given by

$$J = M + \beta T \tag{4.7}$$

Where the consumed fuel for a trip from s_0 to s_1 is obtained by integrating Equation (3.6)

$$M_{fuel} = \int_{s_0}^{s_1} \frac{1}{v} \dot{m}(x, u) ds \tag{4.8}$$

And mission time

$$T = \int_{s_0}^{s_1} \frac{dt}{ds} ds = \int_{0}^{s} \frac{ds}{v(s)} \leq T_{max} \tag{4.9}$$

A gear shift can take place at any time during a mission which of course has an impact on the solution. Modeling for a gear shift scenario can be found in Subsection 4.3.4.

Constraints on the control signals and vehicle dynamics could be included in the problem statement. Here, the control signals are, as mentioned earlier in Chapter 3, fueling and gear. Break is not considered since it is not optimal.

4.2.1 Penalty Parameter

Selecting the penalty parameter β that represents the trade-off between consumed fuel and mission time can be a difficult task, but it is of high importance. The parameter can be viewed as the value that sets the mean velocity $\hat{v}$ for the misson. When β is set to a large value it will generate a high mean speed and a small β value will generate a low mean speed.

The approach taken to calculate an approximation of β is the same one used in Hellström [12]. The process will be outlined below.

For a small distance Δs the model (3.5) can be reformulated using a proportionality constant γ, $[g/J]$, that states the extra fuel ΔM, $[g]$, required to obtain an increase in kinetic energy ΔE_k, $[J]$.

$$\Delta M \approx \gamma \Delta E_k$$

I.e., by using the constant γ kinetic energy can be converted to fuel and vice-versa. So, this relation between fuel and kinetic energy yields the following equation

$$\Delta M = \gamma[\Delta E_k + (F_g + F_a(\hat{v}) + F_r(\hat{v}))\Delta s] \tag{4.10}$$

where ΔM represents consumed fuel and ΔE_k the change in kinetic energy. Given that the constant velocity $\hat{v}$ is the solution for the mission distance S, using Equation (4.10) in combination with $S = \hat{v}T_0$ gives

$$J(\hat{v}) = \gamma(E_k(S) - E_k(0)) + \gamma(F_a(\hat{v}) + F_r(\hat{v}))S + \beta\frac{S}{\hat{v}} \tag{4.11}$$

In a stationary point the derivative of $J(\hat{v})$ will be zero which yields

$$\beta = \gamma\hat{v}^2(F_a'(\hat{v}) + F_r'(\hat{v})) \tag{4.12}$$

So, Equation (4.12) can be used to compute an approximation for the penalty parameter β.

4.3 Look-Ahead Control (LAC)

As mentioned earlier, LAC uses knowledge about the future road topography and computes the optimal velocity profiles for the mission. The following subsections describes the optimization executed by using dynamic programming (DP) and predicting the vehicles behaviour.

4.3.1 Discretization

The OCP (4.6) can be reformulated after discretization

$$\text{minimize} \quad J_N(x_N) + \sum_{k=0}^{N-1} \zeta_k(x_k, u_k) \tag{4.13}$$

where J_N and ζ_k respectively represents terminal cost and step cost respectively. Terminal cost is used to finish in a desired state. Step cost will be elaborated later on.

The mission is divided into N steps with a step length of h_s, each of these discretionary position points are called the stages of the OCP. States and control signals are also discretized, see Figure 4.2. Kinetic energy and fueling are discretized with the step lengths h_{Ek} and h_{uf}. Breaking is never going to be optimal and is therefore not discretized. The gears are already assumed discrete.

4.3.2 Dynamic Programming (DP) Algorithm

Some of the OCP's characteristics are; the dimensions of state space is low, it contains both real and integer variables, and it will be solved for a quite long horizon. As pointed out in Section 2.2.1, low state space dimensions favours the use of DP. The choice of DP as optimization solver is suitable since it finds global optimum for all initial conditions and can handle both non-linearities and constraints. Additionally, the computational complexity grows linearly with the horizon length. So, DP will be used to find a solution to the switching nonlinear mixed-integer problem.

The DP solution to the LAC problem is defined by the following Algorithm (4.14). Feasible states and control signals at stage k are referred to as X_k and U_k. The algorithm works in a backwards manner and makes use of the principle that

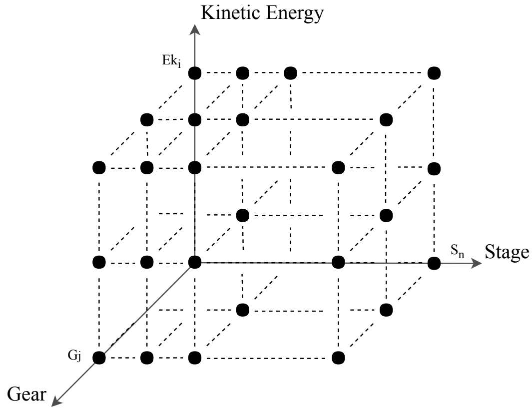

Figure 4.2: *An illustration of the discretization*

if the cost-to-go is known at stage $J_{l\geq n}(x)$ then the cost-to-go at $J_{l=n-1}(x)$ can be derived as a function of $J_{l\geq n}(x)$.

Let $J_N(x) = \tilde{J}_N(x)$ for all $x \in X_N$
For k = N-1, N-2, ..., 0
For $x \in X_k$ let

$$J_k(x) = \min_{u\in U_k}\Big\{\zeta_k(x,u) + J_{k+1}(F_k(x,u))\Big\} \tag{4.14}$$

End for
End for
Output: the course with the optimal cost $J_0(x_0)$

Where $x_{k+1} = F_k(x_k, u_k)$ represent the discretized model. Each feasible state has a corresponding cost-to-go. So at a given position s_l, velocity v_m and gear g the cost-to-go is referred to as $J_l(x) = J_l(s_l, v_m, g)$. The cost-to-go for each state is computed twice. First, under the assumption that no gear shift takes place, $J_{cg}(s_{n-1}, v_m, g)$, and then for the occasion when a gear shift takes place, $J_{gs}(s_{n-1}, v_m, g)$. The states corresponding cost-to-go is then given by minimizing the result from the two scenarios, constant gear and gear shift. Further elaboration regarding the computation for the two scenarios is found in the following sections.

$$J(s_{n-1}, v_m, g) = \min\Big\{J_{cg}(s_{n-1}, v_m, g), J_{gs}(s_{n-1}, v_m, g)\Big\} \tag{4.15}$$

4.3.3 Cost-To-Go and Modeling For Constant Gear

Here, the process to calculate the cost-to-go for a constant gear scenario will be outlined. First, the cost for taking the step from position s_{n-1} to position s_n needs to be calculated. This cost is then added onto the cost-to-go at position s_n. The result is the cost-to-go for position s_{n-1}.

The step-cost is given by

$$\zeta_{cg}(u_k) = \Delta M + \beta \Delta T \tag{4.16}$$

Where the consumed fuel ΔM is derived from Equation (3.6)

$$\Delta M = \int_{s_n}^{s_{n-1}} \dot{m} \frac{ds}{v(s)} \approx \frac{n_{cyl}}{2\pi n_r} \frac{i}{r_w} u_f h_d \tag{4.17}$$

and the required time ΔT is

$$\Delta T = \int_{s_n}^{s_{n-1}} \frac{ds}{v(s)} \approx \frac{h_d}{\frac{v(s_n)+v(s_{n-1})}{2}} \tag{4.18}$$

Here, the velocity at the next stage $v(s_n)$ was calculated using Equation (3.5). the EWL engine model and Euler forward with the distance step length h_d.

Further on, the cost-to-go at position s_n and velocity $v(s_n)$ is acquired through linear interpolation of $J(s_n, v_{k-1}, g)$ and $J(s_n, v_k, g)$, where $v_{k-1} \le v(s_n) \le v_k$. For an illustration of the interpolation see Figure 4.3. The interpolated cost-to-go is represented by J^*.

So, the cost-to-go at the state given by position s_{n-1}, velocity v_m and gear g is found by determining which fueling that minimizes the sum of the step cost and cost-to-go $J^*(s_n, v(s_n), g)$.

$$J_{cg}(s_{n-1}, v_m, g) = \min\Big\{\zeta_{cg}(u_k) + J^*(u_k)\Big\} \tag{4.19}$$

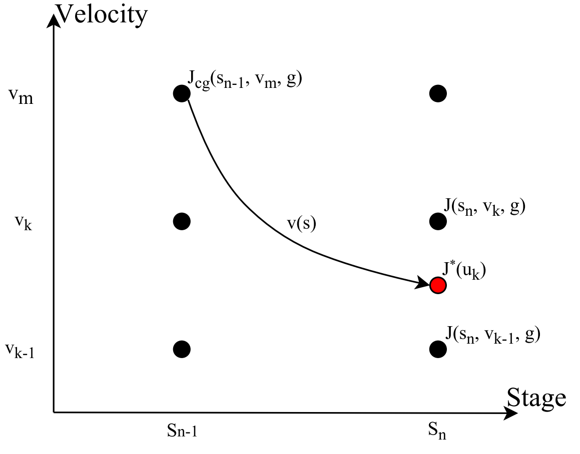

Figure 4.3: *Cost-to-go for constant gear*

4.3.4 Cost-To-Go and Modeling For Gear Shift

Basically the same principle as the one described in Section 4.3.3 is used for a gear shift scenario. However, it is slightly more complicated.

A gear shift was modeled by the required time, distance, change in velocity and consumed fuel. The vehicle is going to freewheel when performing a gear shift from gear g_0 to gear g_1. The constant time, t_{gs}, is the required time for a gear shift and v_0 is the initial velocity. Euler forward and Equation (3.5) gives the velocity after a gear shift

$$v_1 = v_0 + t_{gs}\dot{v}_0 \tag{4.20}$$

When neutral gear is engaged the following is obtained

$$J_e\dot{\omega}_e = M_e = f_e(\omega_e, u_f) \tag{4.21}$$

Since the initial and desired engine speed can be obtained through Equation (3.13). The rotational energy required to synchronize the engine speed during a gear shift together with the amount of fuel to overcome friction can be used to acquire the consumed fuel

$$\Delta m = \gamma \frac{1}{2} J_e(\omega_1^2 - \omega_0^2) + m_{fric}(\omega_e, u_f, t_{gs}) \tag{4.22}$$

Where γ, $[g/J]$, is a proportionality constant, approximately, stating the supplementary fuel needed to receive required increase in kinetic energy [12].

Equation 4.22 together with $\Delta T = t_{gs}$ gives the step-cost for a gear shift

$$\zeta_{gs}(g') = \Delta M + \beta \Delta T \tag{4.23}$$

However, the required distance for a gear shift varies and can be less than the distance step length h_d. The approach taken was to employ constant gear after the gear shift in order to reach the next stage s_n. The required distance for a gear shift can be derived accordingly

$$\Delta s = \int_{v_1}^{v_0} v(t)dt \approx t_{gs}\frac{v_1 + v_0}{2} \tag{4.24}$$

The step-cost $\zeta_{cg}(u_k)$ for the remaining distance $s_{gs,post}$ $(= h_d - \Delta s)$ was acquired is the same way as described in Subsection 4.3.3. The same goes for the cost-to-go at position s_n and velocity $v(s_n)$. Figure 4.4 illustrates the interpolation for a gear shift scenario.

So, when executing a gear shift at the state given by s_{n-1}, v_m and g the cost-to-go is found by determining the fueling and gear that minimizes the sum of the two step costs and cost-to-go $J^*(s_n, v(s_n), g')$, see Equation (4.25).

$$J_{gs}(s_{n-1}, v_m, g) = \min\left\{\zeta_{gs}(g') + \zeta_{cg}(u_k) + J^*(u_k, g')\right\} \tag{4.25}$$

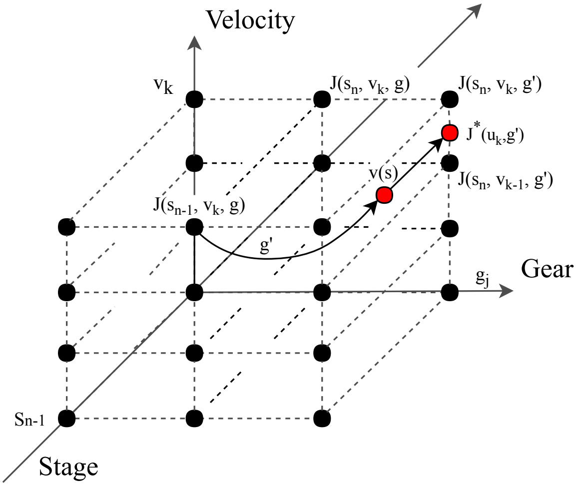

Figure 4.4: *Cost-to-go for gear shift*

4.3.5 Calculating Trajectory

The LAC should feed a velocity profile and desired gear down to the lower level controller. To do so a trajectory must be calculated.

Once the cost-to-go has been computed for the entire discretized horizon, the algorithm should be executed again, but this time in a forward manner. Start at the current position, velocity and gear. Then determine the control signals that results in the lowest cost-to-go at the next stage. The velocity at the next stage will be received. So the procedure can then be repeated at the next stage. Continuing this procedure for the entire horizon will result in a complete trajectory for the vehicle's velocity, gear and control signals.

Assume $J_N(x) = \tilde{J}_N^*(x)$ for all $x \in X_N$
Set $x_{k=0} \in X_0$
For k = 1, 2,..., N-2, N-1

$$J_k(x) = \min_{u \in U_k} \Big\{ \zeta_{k-1}(x, u) + J_k(F_k(x, u)) \Big\} \tag{4.26}$$

End for
Output: complete trajectory for the vehicle's velocity, gear and control signals

4.3.6 Interpolation Boundaries

In order to fulfill e.g. speed constraints, the DP algorithm only runs in between a specified speed interval. However, this causes issues when interpolating at the boundaries of these constraints. The algorithm must be able to handle the possible scenario when it is impossible to find any control signals that takes the vehicle from the current state to a feasible and allowed state in the next stage.

The first solution to be implemented was to set the cost-to-go at the current state to infinity when no feasible control signals could be determined. I.e., make it an unfeasible state. However, this might not always be the case since the state at the next stage might be feasible. Moreover, this approach could potentially make the entire OCP's solution unfeasible when it actually is feasible.

A second solution is to extrapolate the cost-to-go based on the two nearest feasible points. Though, the risk here is that this could assign a low cost-to-go to a state which has no feasible course to the next stage.

A third solution, and the final approach taken, was to add a penalty cost Ω to the interpolation when one of the points is unfeasible. The penalty cost Ω was chosen to be big enough in order to make the algorithm avoid these solutions to the largest extent possible. I.e., the algorithm will deflect from these unfeasible states if there are other feasible states.

4.4 LAC Verification

It was necessary to verify that the LAC performs as expected in terms of finding the optimal solution for a given road profile. So, in order to evaluate the LAC solution, the optimal solution for the given road profile needed to be known beforehand. Here, the simplest engine model, Willans Line Approximation, explained in Section 3.1.3 was used. To this background three tests were designed, explained further below, where the optimal solution was known.

All the tests were designed in such a way that the vehicle should start and finish in the same velocity. After the mission is completed the mean velocity should be the same as the velocity at start and finish. To achieve desired mean velocity, the parameter β had to be tuned. No friction breaks are utilized in the following tests.

Test A is based on that the optimal solution is to maintain constant speed during the entire mission, shown by J. Chang and K. Morlok [17]. Which holds under the condition that it is not allowed to engage neutral gear, i.e. PnG is disabled. Moreover, it is assumed that the HDV is capable of maintaining a constant speed for the entire road profile. A flat road profile was chosen to illustrate and analyze the results in an easy way. The parameters used are presented in Table 4.1 and the plotted results are shown in Figure 4.5. As shown in the Figure, the LAC found the optimal solution and the vehicle is maintaining constant velocity during the entire mission.

The same road profile was used for Test B as for Test A. The only difference compared to Test A was that neutral gear was permitted. The optimal solution in that case should be a PnG strategy, explained earlier in Section 2.2.3. Parameters used in the test are presented in Table 4.1 and plotted results are shown in Figure 4.6. As seen in the figure, the expected optimal solution is found and the vehicle is utilizing a PnG strategy. Noteworthy is the non quadratic behavior of the fuel

Table 4.1: *Parameters used in LAC verification for flat road*

Description	Parameter	Values	Unit
N. of kin. energy disc. points	Ek	60	[J]
Allowed gears (Test A)	g	10-14	[-]
Allowed gears (Test B)	g	1 (N) & 10-14	[-]
N. of fueling disc. points	u_f	280 (0-280)	[mg/cycle]
N. of stage disc. points	s_n	200	[-]
Stage step length	h_s	50	[m]
Max allowed velocity	v_{max}	68.4	[km/h]
Min allowed velocity	v_{min}	90	[km/h]
Desired mean velocity	v_{des}	80	[km/h]
Time penalty (Test A)	β	0.00345	[-]
Time penalty (Test B)	β	0.003285	[-]

injection. Causing this behavior are engine constraints which limits fueling at low velocities. The engine is not able to produce full torque at such low engine speeds, hence the fueling is limited.

Test C consisted of a more challenging road profile compared to the previous tests. Analogous to test A, neutral gear was disabled in order to be able to predict the optimal solution. The road profile consisted of four hills, two uphills and two downhills. The gradient and length of the first pair of hills was constructed in such a way such that the vehicle should not be able to maintain constant velocity. However, the second pair of hills was constructed to enable constant velocity. The parameters used for the test are presented in Table 4.2 and the plotted results are shown in Figure 4.7. As shown in the figure, the vehicle accelerates before the first hill begins and then looses velocity during the uphill. When the plateau is reached it regains desired mean velocity. For the second hill it is a similar behavior, but the inverse since it is a downhill. This behavior is an optimal solution to maintain a specified mean velocity, shown by Fröberg et al. [9]. For the second pair of hills the vehicle maintains constant velocity and as discussed earlier it is the optimal solution to do so.

The LAC solution was implemented in SIMULINK together with the models described in Section 3. Simulations were executed to ensure that the optimal solutions obtained by LAC improves the fuel consumption. The LAC used for the simulation was calculated for a flat road section with the same parameters that was used for Test B in Section 4.4. The WL engine model was used for this case. The solution is presented in Figure 4.6, illustrating PnG behaviour. This solution was compared to driving with a constant velocity corresponding to the mean velocity achieved by the LAC.

The simulation results are presented in Table 4.3 and it shows that the LAC is able to reduce the fuel consumption by 2.29% compared to a conventional CC.

Table 4.2: *Parameters used in LAC verification for hilly road*

Description	Parameter	Value	Unit
N. of kin. energy disc. points	Ek	100	[J]
Allowed gears	g	10-14	[-]
N. of fueling disc. points	u_f	280 (0-280)	[mg/cycle]
N. of stage disc. points	s_n	200	[-]
Stage step length	h_s	50	[m]
Max allowed velocity	v_{max}	97.2	[km/h]
Min allowed velocity	v_{min}	61.2	[km/h]
Desired mean velocity	v_{des}	80	[km/h]
Time penalty	β	0.00345	[-]
Gradient uphill 1	–	3.5	[%]
Gradient downhill 1	–	-1.5	[%]
Gradient uphill 2	–	1.5	[%]
Gradient downhill 2	–	-1	[%]

Table 4.3: *Results for LAC verification compared to CC*

Test	Mean velocity	Fuel consumption	Time in neutral
CC	80 km/h	0.2574 l/km	0 %
LAC	80 km/h	0.2515 l/km (-2.29 %)	63.5 %

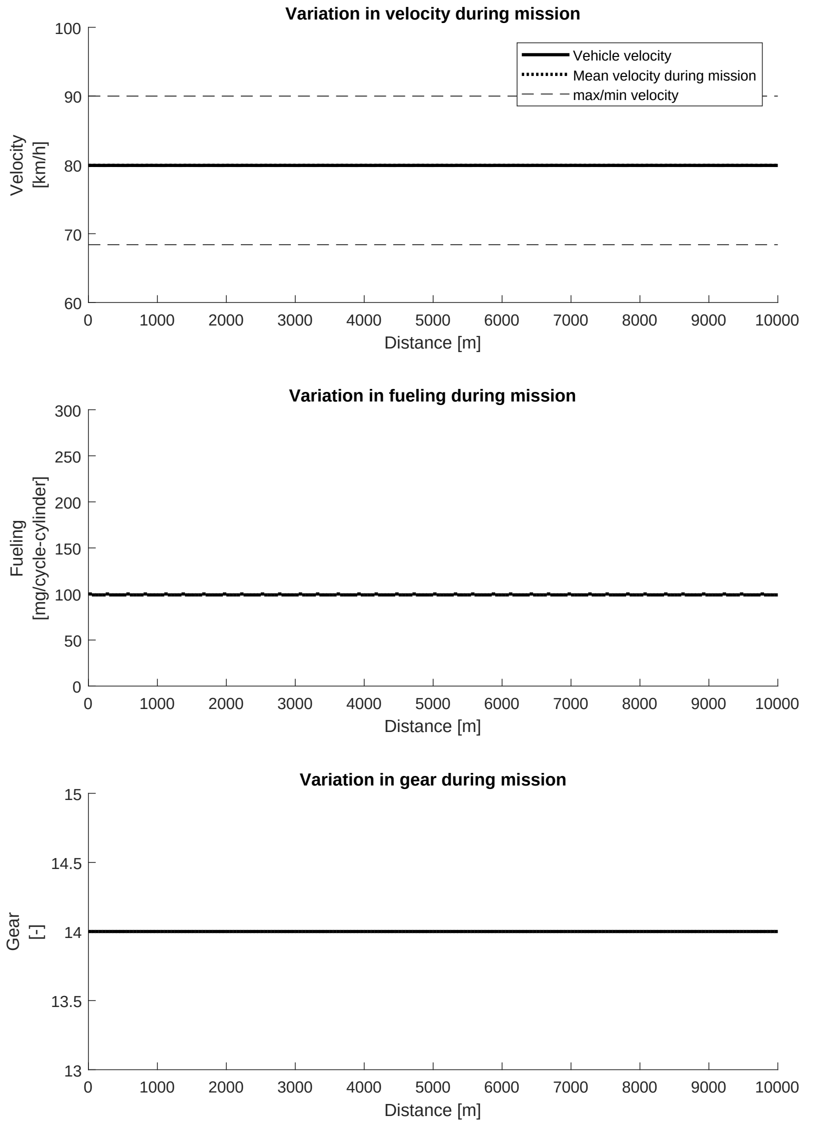

Figure 4.5: *Test A - LAC verification, flat road profile. Start and finish in the same velocity as well as keeping a mean velocity that corresponds to that same velocity. Neutral gear is not allowed.*

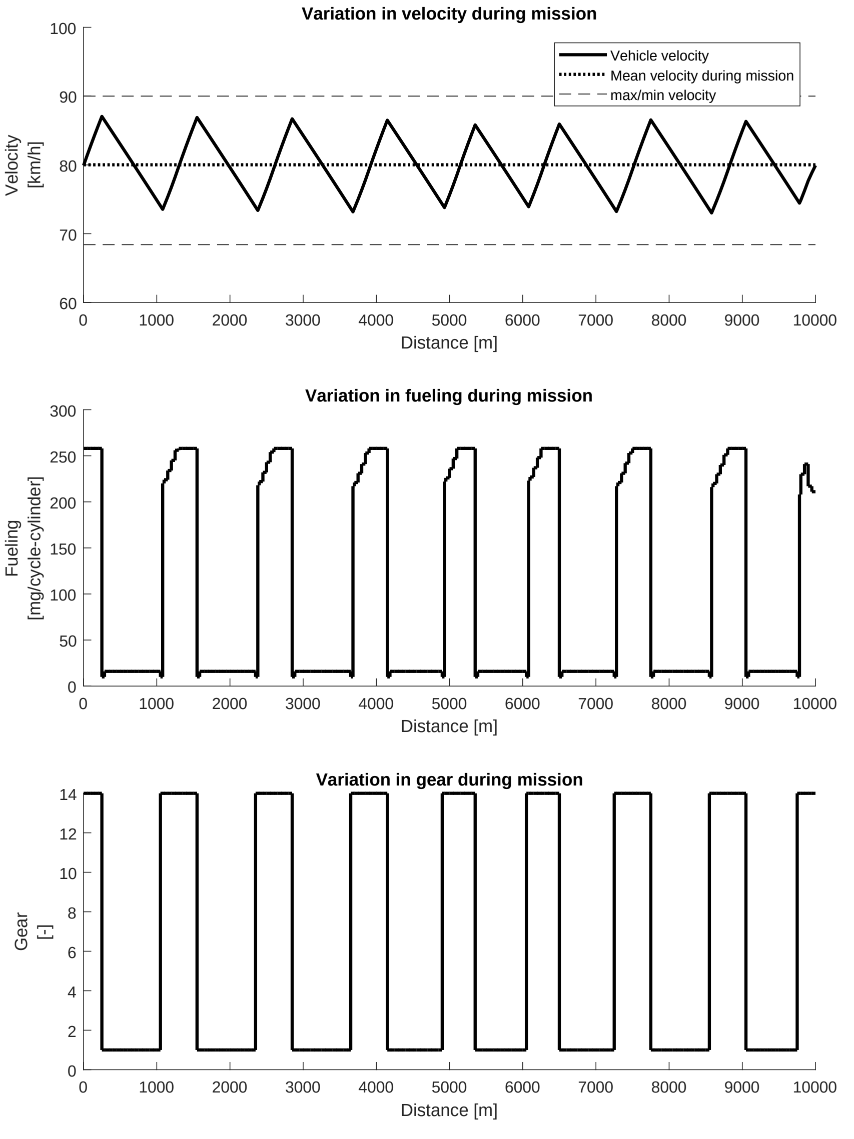

Figure 4.6: *Test B - LAC verification, flat road profile. Start and finish in the same velocity as well as keeping a mean velocity that corresponds to that same velocity. Neutral gear is allowed.*

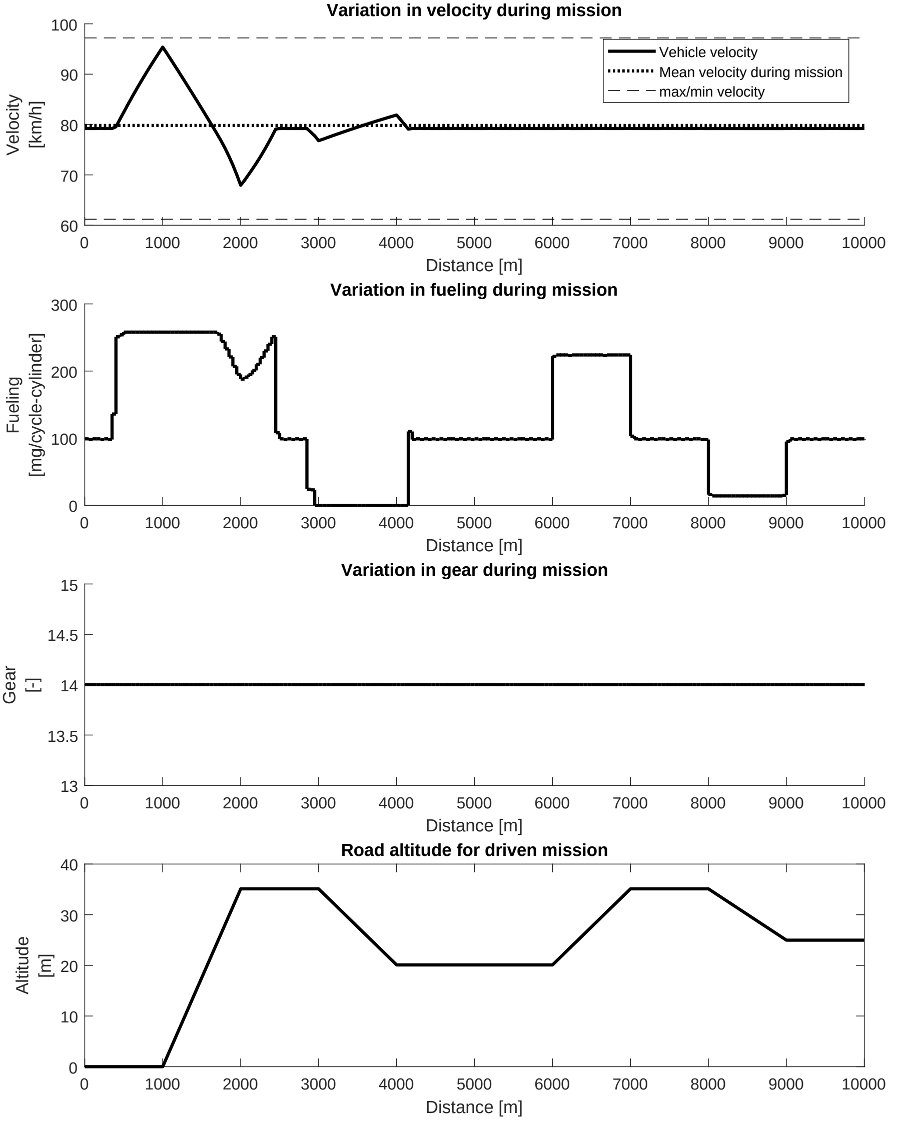

Figure 4.7: *Test C - LAC verification, hilly road profile. Start and finish in the same velocity as well as keeping a mean velocity that corresponds to that same velocity. Neutral gear is not allowed.*

5

Speed Control For Platooning Vehicles

This chapter presents speed controllers and control strategies for vehicles following a preceding vehicle which is utilizing either LAC or solely CC. As pointed out in Section 2.3, there are numerous control strategies for platooning vehicles, and they can be divided into with or without V2V communication.

In this chapter is an Adaptive Cruise Controller (ACC), an Extended Adaptive Cruise Controller (EACC) and an Adaptive Look-Ahead Controller (ALAC) considered and described. ACC does not utilize V2V communication where as EACC and ALAC does. Moreover, the control system architecture when utilizing ALAC is such that the ALAC feeds a velocity profile and desired gear down to lower level control, more specific the EACC.

5.1 Adaptive Cruise Control (ACC)

ACC is an extension of the CC described in Section 4.1. ACC makes use of radar or other sensors to measure the distance to a preceding vehicle, if there is one. Just as a regular CC, the ACC is set to a predefined speed which it maintains if there is no preceding vehicle. However, if there is a preceding vehicle the ACC determines if it is possible (due to safety constraints) to proceed at the desired speed. If it is not possible due to the preceding vehicle moving at a lower speed, or is just too close, the ACC switches from speed control to spacing control.

The ACC described below is autonomous, implying that it relies solely on vehicle sensors and not on wireless communication with other vehicles. The control strategy that was employed for the ACC was adopted from Rajamani [28]. In Rajamani [28, pp. 147] the following is concluded regarding ACC *"[...] constant spacing policy is unsuitable for autonomous control applications."* due to its unstable characteristics. Instead a different spacing policy is suggested; the constant time-gap (CTG) policy. In CTG the desired spacing is not a constant value, but varies linearly with velocity, see equation (5.1).

$$L_{des} = l_{i-1} + hv_i \tag{5.1}$$

Where L_{des} is the desired spacing between the front of the vehicles, l_{i-1} is the length of the preceding vehicle and h is a constant parameter referred to as time-gap. The time-gap is a parameter that is chosen depending on the desired intermediate distance based on e.g. safety margins.

CTG is proven to result in stable behavior as well as string stability. I.e the spacing error will not amplify as it propagates down towards the end of e.g. a vehicle platoon.

The distance between the vehicles is defined by Equation (5.2).

$$\epsilon_i = s_i - s_{i-1} + l_{i-1} \tag{5.2}$$

The spacing error varies with the velocity according to Equation (5.3).

$$\delta_i = \epsilon_i + hv_i \tag{5.3}$$

Based on Equations (5.1) - (5.3) the following controller was adopted from [28, pp. 150]. It is an autonomous control law and represented by (5.4).

$$\ddot{s}_{i\_des} = -\frac{1}{h}(\dot{\epsilon}_i + \lambda\delta_i) \tag{5.4}$$

Where λ is a tuning parameter that puts weight on the spacing error. When desired acceleration is given, desired torque and fuel is handled in the same way as for the CC, see section (4.1).

If the HDV would come too close to preceding vehicle according to a user specified distance (ϵ_{min}), the breaks are activated proportionally to the exceeded minimum distance. Otherwise the braking force is zero, see Equation 5.5. When travelling without a preceding vehicle the braking will act as for the CC, see Equation 4.5.

$$F_b = \begin{cases} 0, & \text{if } (\epsilon_i - \epsilon_{min}) \geq 0 \\ mg_0\mu u_b(\epsilon_i - \epsilon_{min})K_{b,ACC}, & \text{otherwise} \end{cases} \tag{5.5}$$

5.1.1 Verification of ACC

As in the CC case, see Section 4.1.1, the ACC was verified to ensure that it performs as expected when implemented in SIMULINK. The design of the ACC verification test was similar to the one used when verifying the CC, see Section 4.1.1. The lead vehicle received the same velocity reference as in the CC verification and the road profile was identical. The difference was that the lead vehicle had a following vehicle which utilized ACC and had a constant time-gap set at 1. The verification was executed without any limitations on how much the vehicles was allowed to deviate from the reference speed or inter-vehicle spacing restrictions. Which is the reason why the breaks never became active.

As can be seen in Figure 5.1 the intermediate distance has a reference following that is close to perfect, except for the downhill and the negative step in desired velocity. Implying that the ACC works as intended and is able to adapt the inter-vehicle spacing according to the CTG-policy, both for acceleration and slopes. However, as stated there are two cases when the intermediate distance deviates from the reference. In the downhill slope and when the lead vehicle starts to decelerate. It is due to the fact that the breaks are never activated. For the downhill case the lead vehicle is able to maintain a constant velocity of 80 km/h, but the following vehicle is not. It is because the maximum negative engine torque is not enough for the following vehicle to maintain constant velocity due to the reduction in air drag, compared to the lead vehicle. The second case is when the lead vehicle receives a deceleration demand, the fuel injection stops and maximum negative engine torque is used to break. The following vehicle behaves in the same way but since the following vehicle has reduced air drag, the impact caused by resistive forces is less than for the lead vehicle. Similar to the downhill case. Therefore, the following vehicle is not able to decelerate at the same rate as the lead vehicle. However, when the lead vehicle reaches the demanded velocity, the following vehicle quickly adapts to the desired intermediate distance.

5.2 Extended Adaptive Cruise Control (EACC)

In comparison to the conventional ACC, the developed Extended Adaptive Cruise Control (EACC) rely on V2V communication. More specific, the EACC utilizes information regarding preceding vehicles acceleration and thereby makes constant spacing suitable for control applications.

If the state-space representation of a system is given by

$$\begin{aligned} \dot{x} &= Ax + Bu \\ y &= Cx \end{aligned}$$

Utilizing full state feedback $u(t) = -Lx(t)$ for the control signal u and the closed loop system becomes

$$\begin{aligned} \dot{x} &= (A - BL)x \\ y &= Cx \end{aligned}$$

Where the feedback vector L is chosen through pole placement [10].

Here, the states $x(t)$ are given by current intermediate distance ϵ, desired intermediate distance ϵ_{ref}, preceding vehicle's desired velocity $v_{pre,\,ref}$ and the subject vehicle's velocity v

$$x_1(t) = \epsilon(t) - \epsilon_{ref}(t) \tag{5.6a}$$

$$x_2(t) = v(t) - v_{pre,\,ref}(t) \tag{5.6b}$$

State-space representation of the system

$$\dot{x}_1(t) = v_{pre,\ ref}(t) - v(t) = -x_2(t) \tag{5.7a}$$

$$\dot{x}_2(t) = a(t) - a_{pre,\ ref}(t) = \bar{u} \tag{5.7b}$$

Which yields the control law

$$a_{des} = a_{pre,\ ref} + u = a_{pre,\ ref} + k_\epsilon(\epsilon - \epsilon_{ref}) - k_v(v - v_{pre,\ ref}) \tag{5.8}$$

Where k_ϵ and K_v are proportional gain respectively derivative gain. When desired acceleration is retrieved, desired torque and fuel is handled in the same way as for the CC, see section (4.1).

5.2.1 Verification of EACC

As in the CC and ACC case, the EACC had to be verified to ensure that it performed as expected when implemented in SIMULINK. The design of the EACC verification test was similar to the one used when verifying the ACC, see Section 5.1.1. The lead vehicle received the same velocity reference as in the ACC case and the road profile was identical. Instead of a CTG, a fixed distance was used and set at 20 m. The verification was executed without any limitations on how much the vehicle was allowed to deviate from the intermediate distance or spacing restrictions. Which is the reason why the breaks never became active.

As can be seen in Figure 5.2 the intermediate distance has a reference following that is close to perfect, except for the downhill and the negative step in desired velocity. Implying that the EACC works as intended and is able to adapt the inter-vehicle spacing according to the fixed spacing policy for both acceleration and slopes. However, as stated there are two cases when the intermediate distance deviates from the reference. In the downhill slope and when the lead vehicle starts to decelerate. This happens due to the same reasons as for the ACC verification, explained in Section 5.1.1.

5.3 Adaptive Look-Ahead Control (ALAC)

V2V communication enables the deployment of Adaptive Look-Ahead Control (ALAC). Here, V2V communication implies that the preceding vehicle is feeding its velocity trajectory to the following vehicle in the platoon. ALAC optimizes the velocity profile for the following vehicle based on the precomputed velocity trajectory of the preceding vehicle.

The solution to the optimal control problem is derived in the same manner and using the same algorithms as for LAC, see Section 4.3. I.e., the cost-to-go is computed in the same way, for both constant gear and gear shift. The only differences is that a fourth dimension is introduced and the cost-to-go is obtained through bilinear interpolation.

A platoon is in place the vehicle motion is computed as a function of intermediate distance, see Section 3.2. Additionally, constraints on minimum intermediate distance is set in the optimization problem in order to avoid a collision.

5.3.1 Intermediate Distance

The intermediate distance, ϵ, between two vehicles was introduced earlier in Section 5.1.

$$\epsilon = s_{pre} - s$$

Here, s_{pre} and s represents the positions of the preceding respectively following vehicle. Differentiation with respect to the following vehicle's position gives

$$\frac{d\epsilon}{ds} = \frac{ds_{pre}}{ds} - \frac{ds}{ds} = \frac{v_{pre}(s+\epsilon)}{v(s)} - 1 \tag{5.9}$$

Where v_{pre} represents the optimal velocity trajectory for the preceding vehicle. After discretization, the intermediate distance can be computed utilizing Euler forward and the distance step length

$$\epsilon_{k+1} = \epsilon_k + h_s\left(\frac{v_{pre}(s_k+\epsilon_k)}{v(s_k)} - 1\right) \tag{5.10}$$

Introducing a constant intermediate distance reference, ϵ_{ref}, which the following vehicle needs to relate to. Deviation d from this intermediate distance reference can be derived as

$$d = \epsilon - \epsilon_{ref} \tag{5.11}$$

$$\frac{dd}{ds} = \frac{d\epsilon}{ds} - \frac{d\epsilon_{ref}}{ds} = \frac{d\epsilon}{ds} \tag{5.12}$$

Together with equation 5.9 gives

$$d_{k+1} = d_k + h_s\left(\frac{v_{pre}(s_k+d_k+\epsilon_{ref})}{v(s_k)} - 1\right) \tag{5.13}$$

Intermediate distance deviation, d, was added as the additional state to the discretization described in Section 4.3. I.e. a fourth dimension was implemented, see Figure 5.3 for an illustration.

5.3.2 Bilinear Interpolation

For LAC the cost-to-go is obtained through linear interpolation and the procedure was described earlier in Section 4.3. However, when using ALAC the cost-to-go at position s_n, velocity $v(s_n)$, gear g and intermediate distance deviation $d(s_n)$ is acquired through bilinear interpolation. For both the constant gear and gear shift scenario, see Figure 5.4 and 5.5.

5.4 ALAC verification

It was necessary to verify that the ALAC performs as expected in terms of finding the optimal solution when adapting to the preceding vehicles trajectory. So, in order to evaluate the ALAC solution, the optimal solution needed to be known beforehand. Here, the simplest engine model was used, Willans Line Approximation, explained in Section 3.1.3. To this background a test was designed, explained further below.

The test was designed in such a way that the vehicle should start and finish with the same velocity and intermediate distance to preceding vehicle. Hence, there is no need to tune the parameter β since the mean velocity will be the same as for the preceding vehicle. No friction breaks are used in the following test.

The preceding vehicle maintains constant velocity during a complete mission. The optimal solution for the subject vehicle is to keep as short intermediate distance as possible during the entire mission. Determined by a minimum allowed distance. Which holds under the condition that it is not allowed to engage neutral gear, i.e. PnG is disabled. Moreover, it is assumed that the subject HDV is capable of maintaining a constant speed for the entire road profile. A flat road profile was chosen to illustrate and analyze the results in an easy way. The parameters used are presented in Table 5.1 and the plotted results are shown in Figure 5.6. As shown in the Figure, the ALAC finds the optimal solution and the vehicle is minimizing the intermediate distance. Moreover, the velocity is kept constant for the entire mission except at the beginning and end where the vehicle has to keep a specified distance.

Table 5.1: *Parameters used in ALAC verification for flat road*

Description	Parameter	Values	Unit
N. of kin. energy disc. points	Ek	50	[J]
Allowed gears (Test A)	g	10-14	[-]
N. of fueling disc. points	u_f	280 (0-280)	[mg/cycle]
N. of stage disc. points	s_n	200	[-]
N. of interm. dist. disc. points	ϵ_n	61	[-]
Stage step length	h_s	50	[m]
Max allowed velocity	v_{max}	72	[km/h]
Min allowed velocity	v_{min}	90	[km/h]
Intermediate dist. - start & finish	ϵ_{des}	5	[m]
Min allowed intermediate dist.	ϵ_{min}	5	[m]
Max allowed intermediate dist.	ϵ_{max}	20	[m]

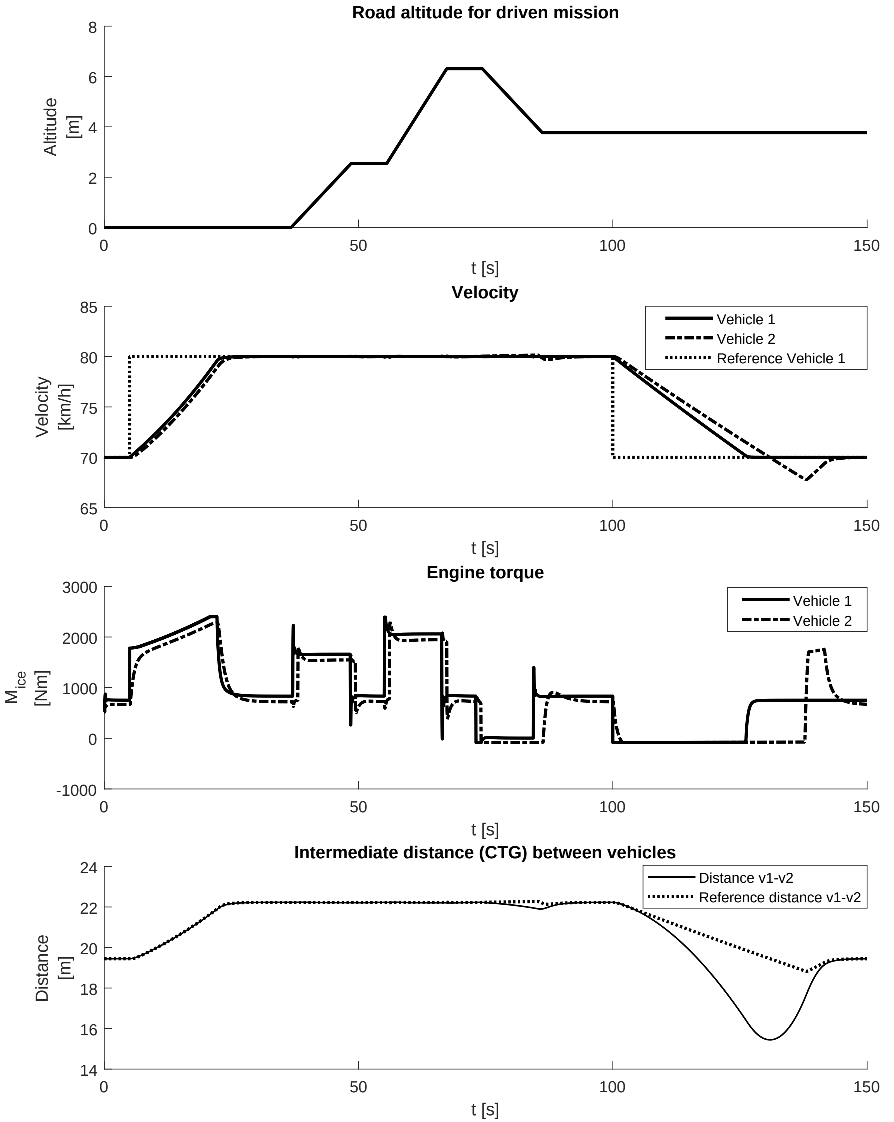

Figure 5.1: *Verification of ACC, including one positive step in velocity, three different road slopes and one negative step in velocity. Bottom plot shows how the intermediate distance varies during the driven mission, CTG is set at 1.*

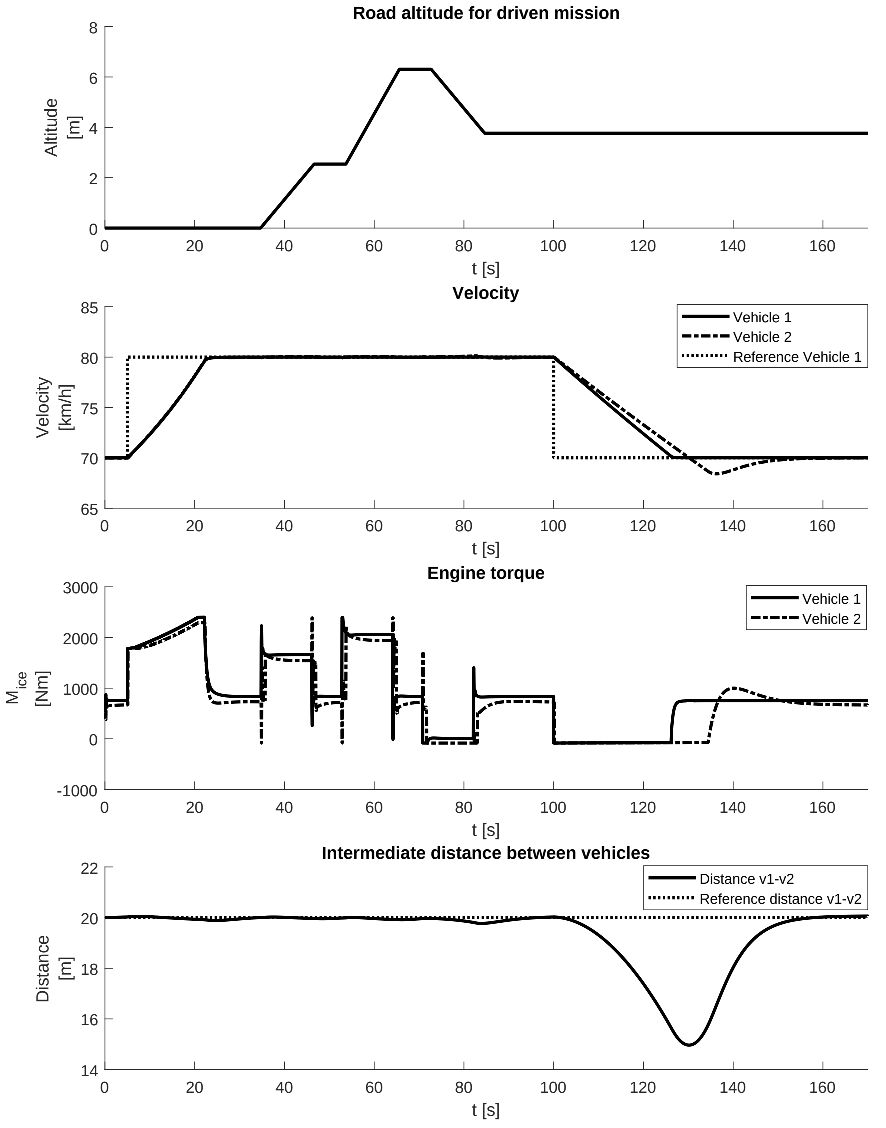

Figure 5.2: *Verification of EACC, including one positive step in velocity, three different road slopes and one negative step in velocity. Bottom plot shows how the intermediate distance varies during the driven mission, intermediate distance reference is set at 20m .*

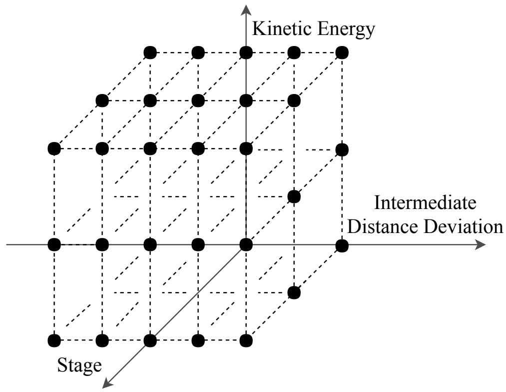

Figure 5.3: *An illustration of the discretization when only one gear is enabled.*

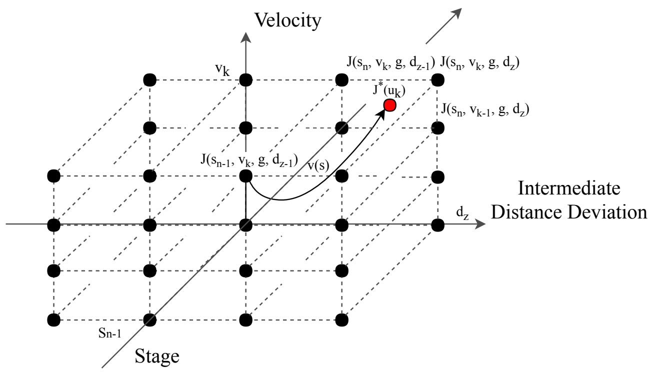

Figure 5.4: *Computing cost-to-go for constant gear using bilinear interpolation for ALAC.*

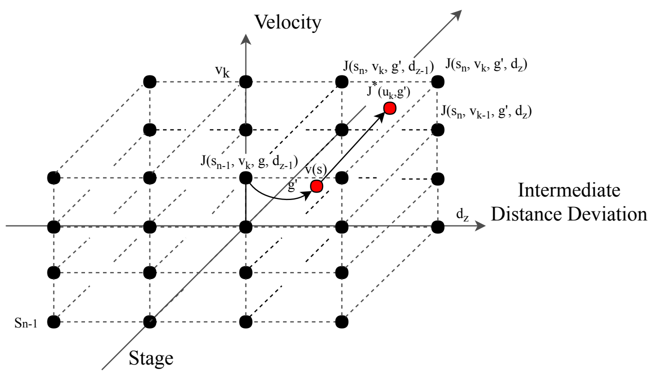

Figure 5.5: *Computing cost-to-go for gear shift using bilinear interpolation for ALAC.*

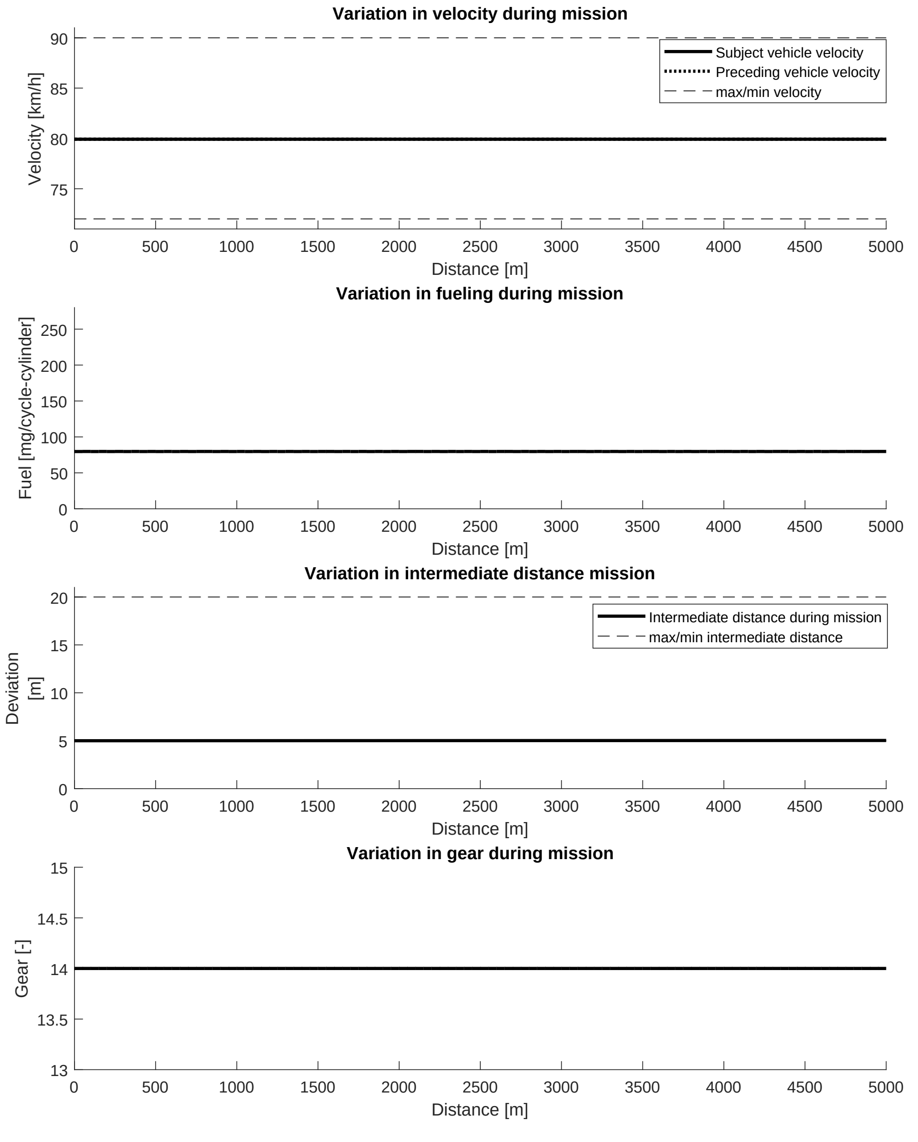

Figure 5.6: *Verification of ALAC, flat road profile. Start and finish in the same velocity and intermediate distance. Neutral gear is not allowed.*

6

Simulation Results

Simulation results from different mission scenarios will be presented in this Chapter. The deployed control strategy for each scenario will be outlined and the numerical optimization was made with the EWL. It should be mentioned that each vehicle has a mass of 40 ton, the mean velocity for all vehicles is 80 km/h and the minimum intermediate distance allowed is 5 meter.

6.1 Road Topography - Flat road

The road topography for this scenario is a five kilometer flat road. Control strategy, fuel consumption and time spent in neutral gear for each vehicle, and scenario, can be found in Table 6.1 - 6.3. The velocity and intermediate distance profiles related to Table 6.1 are illustrated in Figure 6.1. See Appendix A.1 for profiles related to results presented in the other tables.

Table 6.1: *Simulation results for a platoon consisting of 2 vehicles on a flat road. The EWL engine model was used when simulating.*

Ctrl. Strat. (HDV_i, HDV_{i+1})	**Fuel Cons. [%] per HDV**	**% in Neutral per HDV**	**Fuel Cons. [%] Platoon avg.**
CC (nominal)	100.0	0.0	100.0
LAC, ACC	97.1, 85.3	0.0, 0.0	91.2
LAC, ALAC	97.1, 85.3	0.0, 0.0	91.2
LAC, ALAC*	98.3, 83.4	0.0, 56.9	90.9
LAC*, ALAC	95.0, 85.3	59.8, 0.0	90.2
LAC*, ALAC*	96.2, 83.5	59.8, 58.8	89.9

* implies that PnG is allowed

Table 6.2: *Simulation results for a platoon consisting of 2 vehicles on a flat road. The MVEM engine model was used when simulating.*

Ctrl. Strat. (HDV_i, HDV_{i+1})	**Fuel Cons. [%] per HDV**	**% in Neutral per HDV**	**Fuel Cons. [%] Platoon avg.**
CC (nominal)	100.0	0.0	100.0
LAC, ALAC	97.0, 85.3	0.0, 0.0	91.2
LAC*, ALAC*	97.5, 84.6	59.7, 58.8	91.1

* implies that PnG is allowed

Table 6.3: *Simulation results for a platoon consisting of 3 vehicles on a flat road. The EWL engine model was used when simulating.*

Ctrl. Strat. $(HDV_i, HDV_{i+1}, HDV_{i+2})$	**Fuel Cons. [%] per HDV**	**% in Neutral per HDV**	**Fuel Cons. [%] Platoon avg.**
CC (nominal)	100.0	0.0	100.0
LAC, ALAC, ALAC	97.1, 85.3, 82.2	0.0, 0.0, 0.0	88.2
LAC*, ALAC*, ALAC*	96.1, 81.2, 77.7	59.8, 59.8, 59.8	85.0

* implies that PnG is allowed

6.2 Road Topography - Uphill

The road topography for this scenario is a 2.3 kilometer road with a 3 % uphill slope lasting for 300 meters. Control strategy, fuel consumption and time spent in neutral gear for each vehicle, and scenario, can be found in Table 6.4 - 6.6. The velocity and intermediate distance profiles related to Table 6.4 are illustrated in Figure 6.2 and 6.3. See Appendix A.1 for profiles related to results presented in the other tables.

Table 6.4: *Simulation results for a platoon consisting of 2 vehicles driving uphill. The EWL engine model was used when simulating.*

Ctrl. Strat. (HDV_i, HDV_{i+1})	**Fuel Cons. [%] per HDV**	**% in Neutral per HDV**	**Fuel Cons. [%] Platoon avg.**
CC (nominal)	100.0	0.0	100.0
LAC, ACC	97.4, 88.5	0.0, 0.0	93.0
LAC, ALAC	97.4, 84.3	0.0, 0.0	90.9
LAC, ALAC*	98.0, 83.0	0.0, 35.3	90.5
LAC*, ALAC	96.4, 84.7	46.0, 0.0	90.6
LAC*, ALAC*	96.8, 83.6	46.0, 40.8	90.2

* implies that PnG is allowed

Table 6.5: *Simulation results for a platoon consisting of 2 vehicles driving uphill. The MVEM engine model was used when simulating.*

Ctrl. Strat. (HDV_i, HDV_{i+1})	**Fuel Cons. [%] per HDV**	**% in Neutral per HDV**	**Fuel Cons. [%] Platoon avg.**
CC (nominal)	100.0	0.0	100.0
LAC, ALAC	98.0, 85.0	0.0, 0.0	91.5
LAC*, ALAC*	98.0, 85.2	46.1, 49.5	91.6

* implies that PnG is allowed

Table 6.6: *Simulation results for a platoon consisting of 3 vehicles driving uphill. The EWL engine model was used when simulating.*

Ctrl. Strat. (HDV_i, HDV_{i+1}, HDV_{i+2})	**Fuel Cons. [%] per HDV**	**% in Neutral per HDV**	**Fuel Cons. [%] Platoon avg.**
CC (nominal)	100.0	0.0	100.0
LAC, ALAC, ALAC	97.2, 84.4, 80.9	0.0, 0.0, 0.0	87.5
LAC*, ALAC*, ALAC*	96.6, 83.5, 79.4	46.0, 39.5, 41.7	86.5

* implies that PnG is allowed

6.3 Road Topography - Downhill

The road topography for this scenario is a 2.3 kilometer road with a 3 % downhill slope lasting for 300 meters. Control strategy, fuel consumption and time spent in neutral gear for each vehicle, and scenario, can be found in Table 6.7 - 6.9. The velocity and intermediate distance profiles related to Table 6.7 are illustrated in Figure 6.4 and 6.5. See Appendix A.1 for profiles related to results presented in the other tables.

Table 6.7: *Simulation results for a platoon consisting of 2 vehicles driving downhill. The EWL engine model was used when simulating.*

Ctrl. Strat. (HDV_i, HDV_{i+1})	**Fuel Cons. [%] per HDV**	**% in Neutral per HDV**	**Fuel Cons. [%] Platoon avg.**
CC (nominal)	100.0	0.0	100.0
LAC, ACC	96.1, 75.1	0.0, 0.0	85.6
LAC, ALAC	94.6, 71.5	0.0, 0.0	83.1
LAC, ALAC*	96.4, 67.3	0.0, 50.2	81.8
LAC*, ALAC	94.0, 70.7	75.8, 0.0	82.4
LAC*, ALAC*	94.0, 67.9	75.8, 24.1	81.0

* implies that PnG is allowed

Table 6.8: *Simulation results for a platoon consisting of 2 vehicles driving downhill. The MVEM engine model was used when simulating.*

Ctrl. Strat. (HDV_i, HDV_{i+1})	**Fuel Cons. [%] per HDV**	**% in Neutral per HDV**	**Fuel Cons. [%] Platoon avg.**
CC (nominal)	100.0	0.0	100.0
LAC, ALAC	95.5, 72.9	0.0, 0.0	84.2
LAC*, ALAC*	94.2, 69.9	75.8, 24.1	82.1

* implies that PnG is allowed

Table 6.9: *Simulation results for a platoon consisting of 3 vehicles driving downhill. The EWL engine model was used when simulating.*

Ctrl. Strat. (HDV_i, HDV_{i+1}, HDV_{i+2})	**Fuel Cons. [%] per HDV**	**% in Neutral per HDV**	**Fuel Cons. [%] Platoon avg.**
CC (nominal)	100.0	0.0	100.0
LAC, ALAC, ALAC	94.8, 70.1, 65.1	0.0, 0.0, 0.0	76.7
LAC*, ALAC*, ALAC*	93.9, 68.0, 57.8	75.9, 24.3, 41.5	73.2

* implies that PnG is allowed

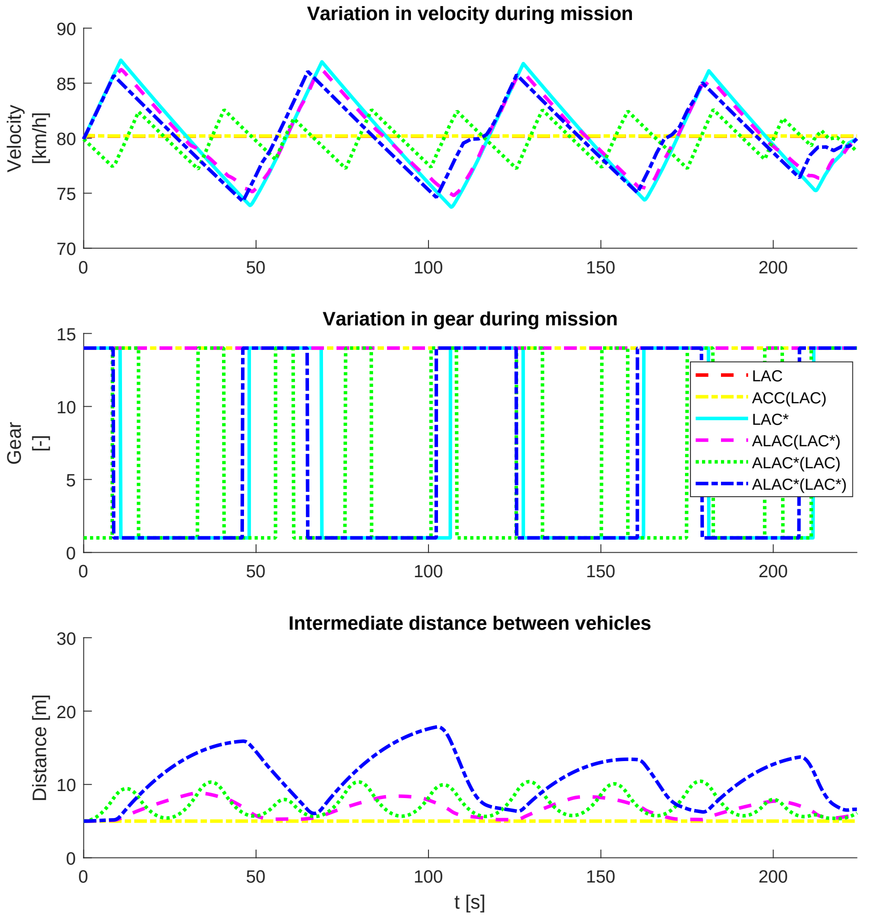

Figure 6.1: *Velocity, intermediate distance and gear profiles when simulating a platoon consisting of 2 vehicles on a flat road. Different control strategies were applied. * implies that PnG is allowed and the lead vehicles control strategy is stated within the parentheses.*

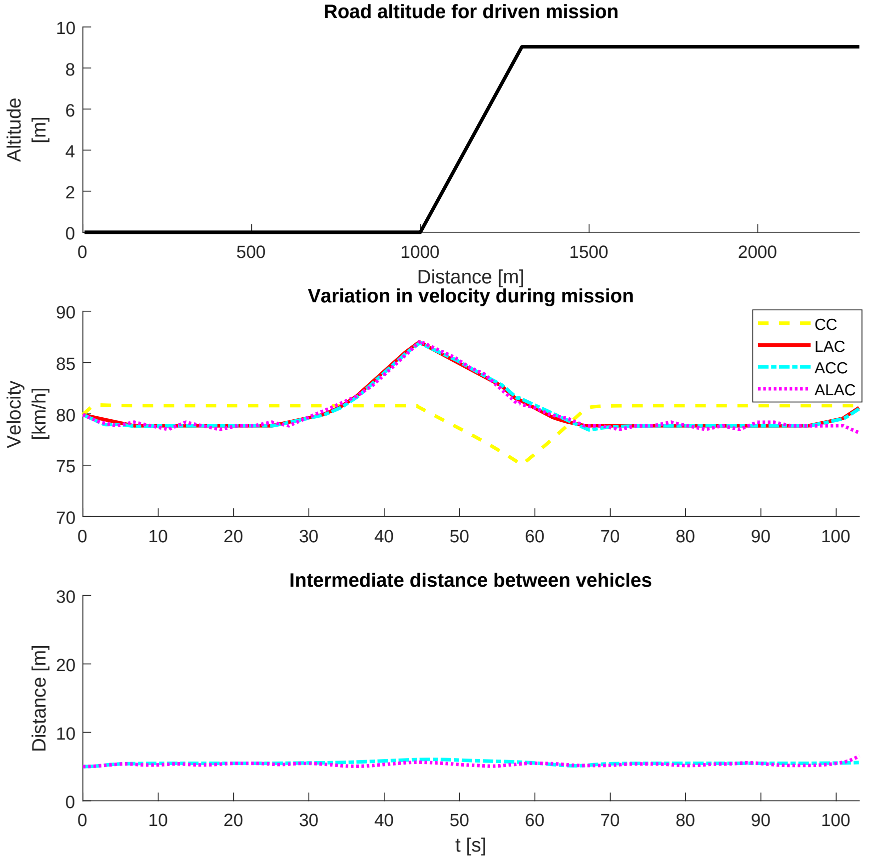

Figure 6.2: *Velocity and intermediate distance profiles when simulating a platoon consisting of 2 vehicles driving uphill. Different control strategies were applied. PnG was not allowed.*

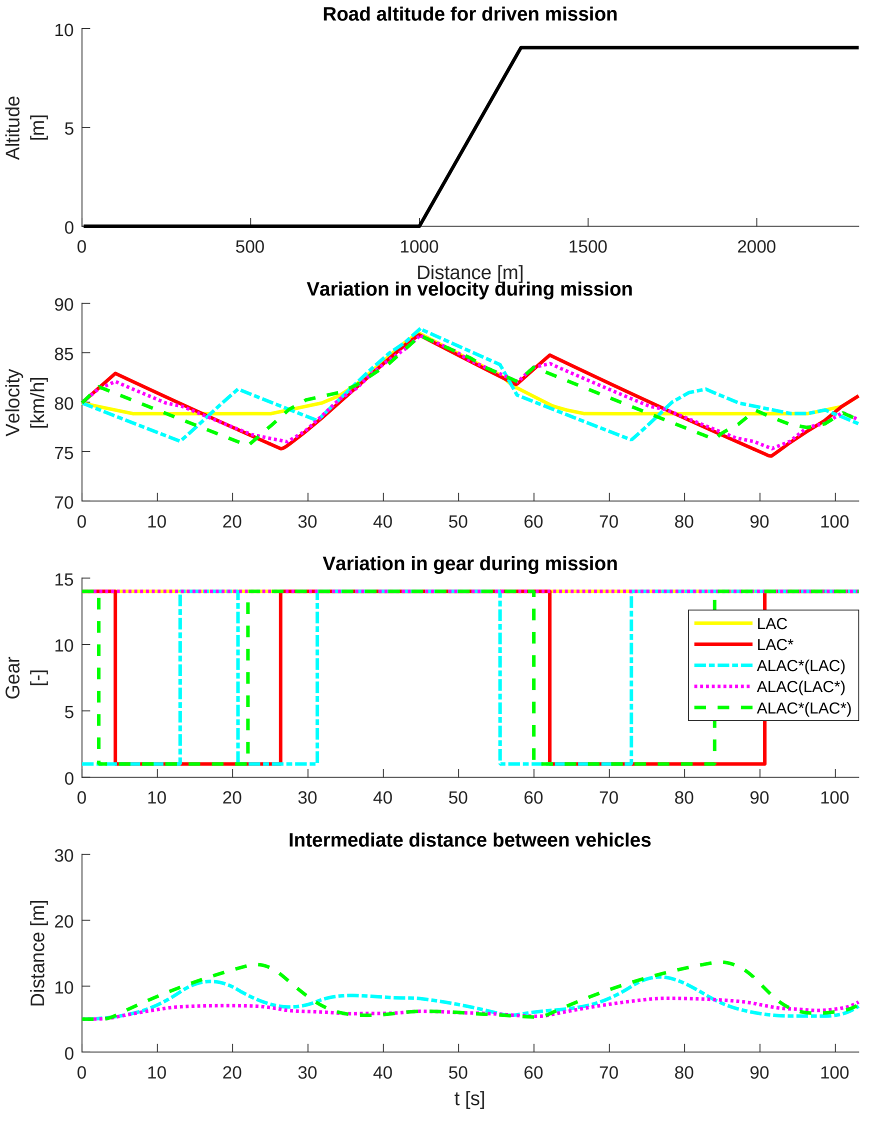

Figure 6.3: *Velocity, intermediate distance and gear profiles when simulating a platoon consisting of 2 vehicles driving uphill. Different control strategies were applied. * implies that PnG is allowed and the lead vehicles control strategy is stated within the parentheses.*

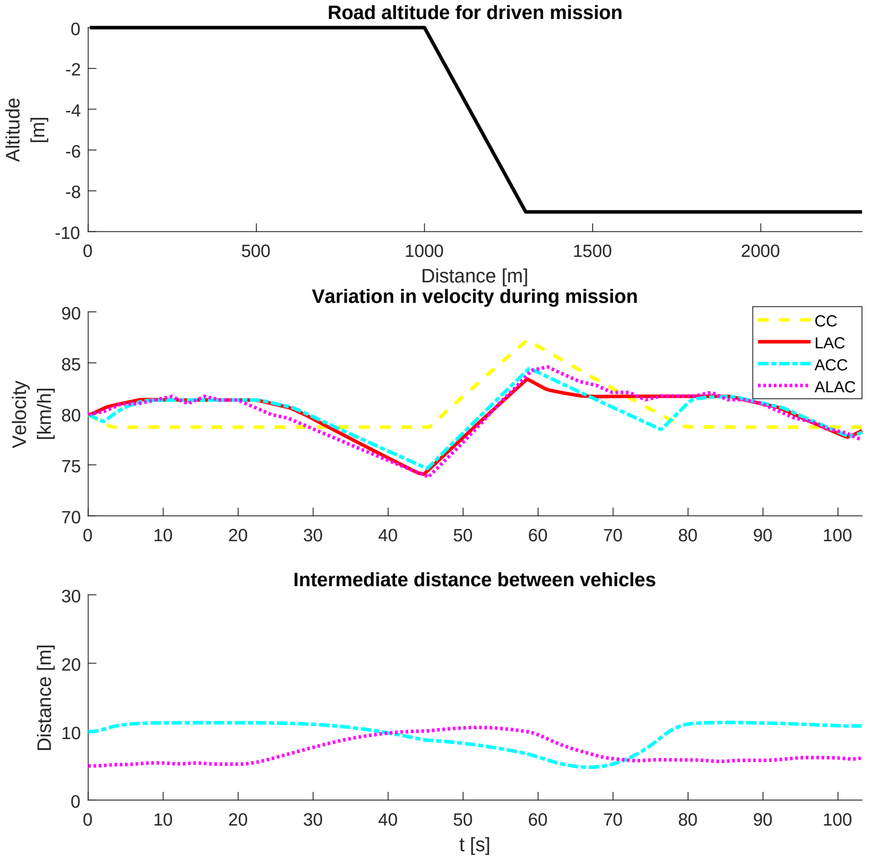

Figure 6.4: *Velocity and intermediate distance profiles when simulating a platoon consisting of 2 vehicles driving downhill. Different control strategies were applied. PnG was not allowed.*

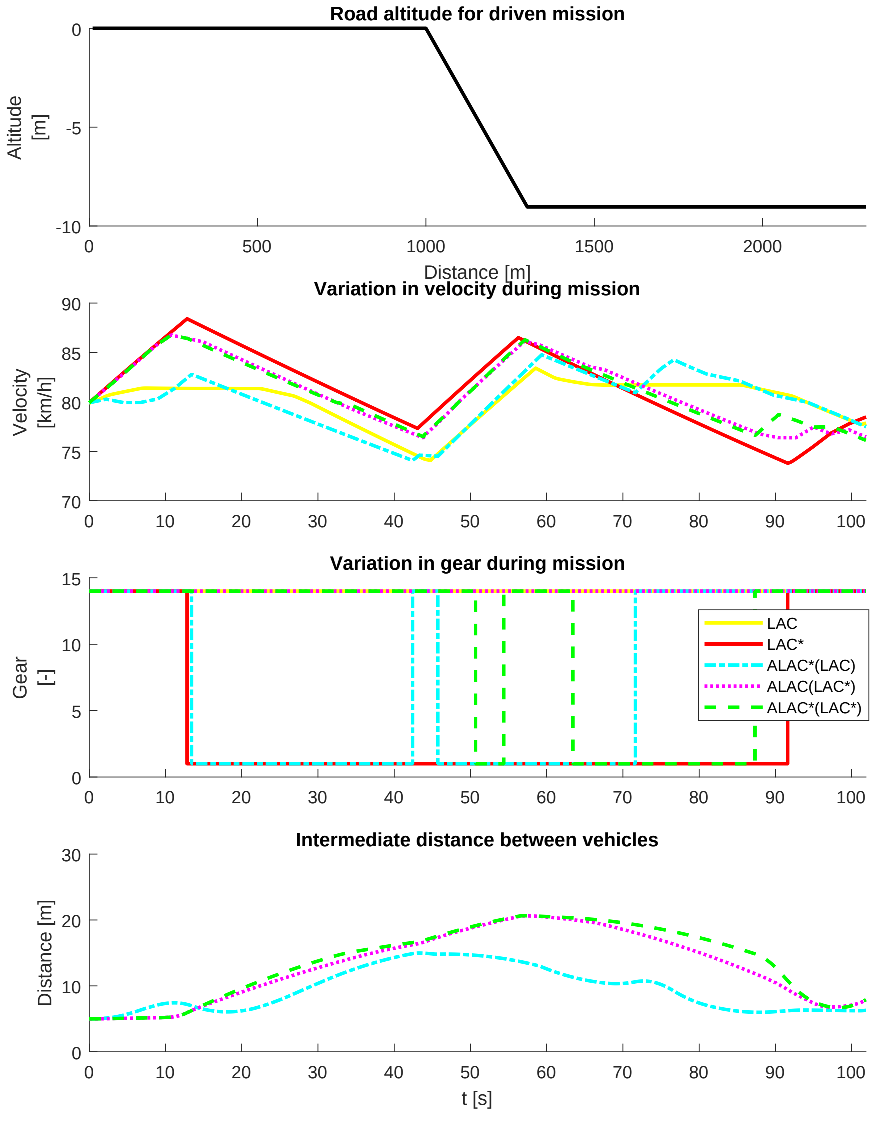

Figure 6.5: *Velocity, intermediate distance and gear profiles when simulating a platoon consisting of 2 vehicles driving downhill. Different control strategies were applied. * implies that PnG is allowed and the lead vehicles control strategy is stated within the parentheses.*

7
Summary

Summary of the thesis will be presented in this section. First, there is a discussion of the results. Thereafter a conclusion, relating to the purpose and expected results and last, suggestions for future work.

7.1 Discussion

The results presented in Section 6 strongly supports the claims that platooning in combination with information about future road topography and V2V communication can reduce the fuel consumption significantly.

The most significant change in fuel reduction is achieved for the second and third vehicle in the platoon. This holds for all three road profiles which implies that the greatest change in fuel reduction comes from air drag reduction and not information about the future road topography. However, the fuel reduction can not solely be derived from air drag reduction but also from the LAC and optimization of velocity trajectory. When combining LAC with ALAC, enabled through V2V communication, the results improve even further. The ALAC is planning its velocity and intermediate distance in the most favourable way.

An interesting comparison can be made between the conventional ACC and the ALAC. ACC applies a CTG-policy and the ALAC utilizes V2V communication to optimize intermediate distance and velocity. An improvement in fuel consumption is clearly seen for the individual vehicles when driving a two vehicle platoon with LAC in combination with ALAC, in comparison to driving LAC combined with ACC. It brings on an overall reduction of fuel for the entire platoon. The reason to why there is no difference for the flat segment is that the conventional ACC solution is optimal, as previously discussed, so therefore the ALAC solution is equivalent.

These results confirm that the developed ALAC is at its minimum better than a conventional ACC and is an improvement of the ALAC proposed by Alam [2].

The aim was i.a. to study the potential of reducing fuel consumption by applying a PnG strategy instead of maintaining constant gear throughout the entire mission. The results show that PnG reduces the consumption of fuel. Compared to constant gear the results indicate that PnG can reduce the fuel consumption for the entire platoon with roughly 1-3 %, compared to the nominal case (LAC and ALAC is used by all vehicles). Which is reasonable since it is of the same magnitude as for an individual vehicle.

When simulating three vehicles, two cases (apart from the nominal case) were selected based on the results for two vehicles and reproduced. First, the case when the lead vehicle utilized LAC in constant gear and two following vehicles ALAC in constant gear. Second, the case when the lead vehicle utilized LAC combined with PnG and the two following vehicles ALAC combined with PnG. The results are similar to the results for the two vehicle case. However, the third vehicle have an even larger fuel consumption reduction compared to the second vehicle, as expected. Which of course generates a significantly lower fuel consumption for the platoon as a whole. This again strengthens the incentive to utilize platooning.

The EWL engine model was used when performing the simulations discussed above. So, there was a need to test if the fuel consumption results would hold even when using the more sophisticated MVEM engine model in simulations. The results show a slightly higher fuel consumption when the MVEM model is used. Which is intuitive since the optimization was done with the EWL model and not with the MVEM model. It should also be noted that the PnG strategy does not result in a significant reduction in fuel consumption compared to maintaining constant gear anymore. For the uphill case it is even more beneficial to maintain constant gear throughout the mission.

The greatest potential in fuel reduction is seen for the downhill segment where the reduction for an individual vehicle is as high as 42.2 %, compared to the nominal case (CC). The potential in fuel reduction for the flat and uphill segment are similar to each other. The reduction for an individual vehicle is as high as 22.3 % and 20.6 % respectively. Since a road topography is constantly varying the important thing is that it gives an improvement in efficiency for all types of road segments. Which is fulfilled.

7.2 Conclusion

The main objective of this thesis was to study how platooning vehicles and PnG interact when pursuing lower fuel consumption. To do so a model of the platoon and optimization-based controllers were designed and developed. A Look-Ahead Controller (LAC) algorithm and Adaptive Look-Ahead Controller (ALAC) algorithm.

The most suitable strategy, in terms of fuel consumption, for the platoon as a whole is closely related to the one for individual vehicles. The strategies where the highest individual fuel reduction is achieved for a single vehicle is also where the highest total fuel reduction is achieved for the entire platoon. A lead vehicle should utilize both LAC and PnG, the other platooning vehicles should employ ALAC to also utilize PnG meanwhile keeping a short intermediate distance.

For all the studied cases it can be concluded that there is a reduction in fuel consumption when a PnG strategy is utilized, compared to maintaining a constant gear throughout the mission. However, it has to be considered that the PnG strategy does have some disadvantages. The increased wear of components when constantly shifting gears as well as the driving comfort when having a continuous acceleration or deceleration. When taking these aspects into consideration it might be worth considering to not use the PnG strategy to benefit other metrics.

The fuel consumption is slightly higher when using the sophisticated MVEM engine model in simulations. However, the general idea of a significant reduction in fuel consumption still holds even though the optimization was done with the EWL engine model.

7.3 Future Work

There are several interesting aspects open for investigation in future work. Foremost, the impact of hybridization and its possibilities to further reduce fuel consumption.

Moreover, it is desirable to dig deeper into how the engine models' sophistication degree, used for numerical optimization, affects the fuel reduction. I.a., study its impact when the driveline components are not assumed stiff in simulation.

Furthermore, it is suitable to complete a more thorough investigation on the usage of the ALAC Algorithm when there are more than 2 platooning vehicles. In order to confirm the possibilities of this particular ALAC approach.

Regarding the ALAC algorithm, it would be beneficial to introduce deviation from preceding vehicles kinetic energy as a new state, instead of solely kinetic energy. I.e., implement the approach used for intermediate distance on kinetic energy as well. It would enable a tighter grid with less computational complexity, compared to the algorithm used in this thesis.

To enable implementation on real trucks and validation of results against measured data from real-life experiments as a next step, the computational requirements of the the algorithms' has to be reduced. Computational requirements were not taken under consideration in this thesis so there is room for improvements.

Of course must sensitivity to traffic, impact on surroundings, safety measures etc. be investigated and considered before conducting real-life experiments. Since, ALAC can adapt to preceding vehicle the prospects are promising.

Another aspect that is interesting to study is how the vehicles should be positioned in the platoon when they are from different companies. Since it is most beneficial to be second or third it could arise conflict where no one wants to be the lead vehicle. This could open up for a centralized system for competing companies, which balances out the fuel cost so that the saving for each vehicle becomes equal.

Finally it would be of interest to study how a cooperative approach, where all vehicles are allowed to utilize PnG, would perform. Where the optimization would be done for the platoon as a whole, including different vehicle parameters.

Appendix

A
Additional

This chapter contains additional material that supports the reports analysis and conclusions.

A.1 Appendix 1

The figures in this section illustrates the velocity and intermediate distance profiles that belong to the simulation results presented in Table 6.3, 6.6 and 6.9.

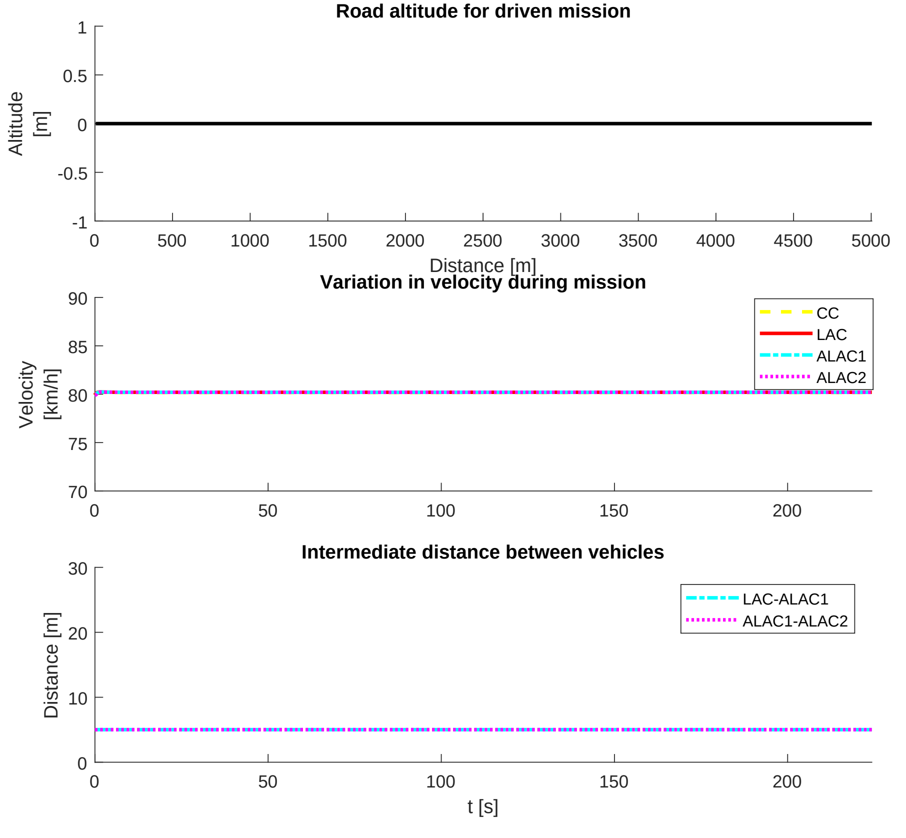

Figure A.1: *Velocity and intermediate distance profiles when simulating 3 vehicles on flat road. PnG is not allowed.*

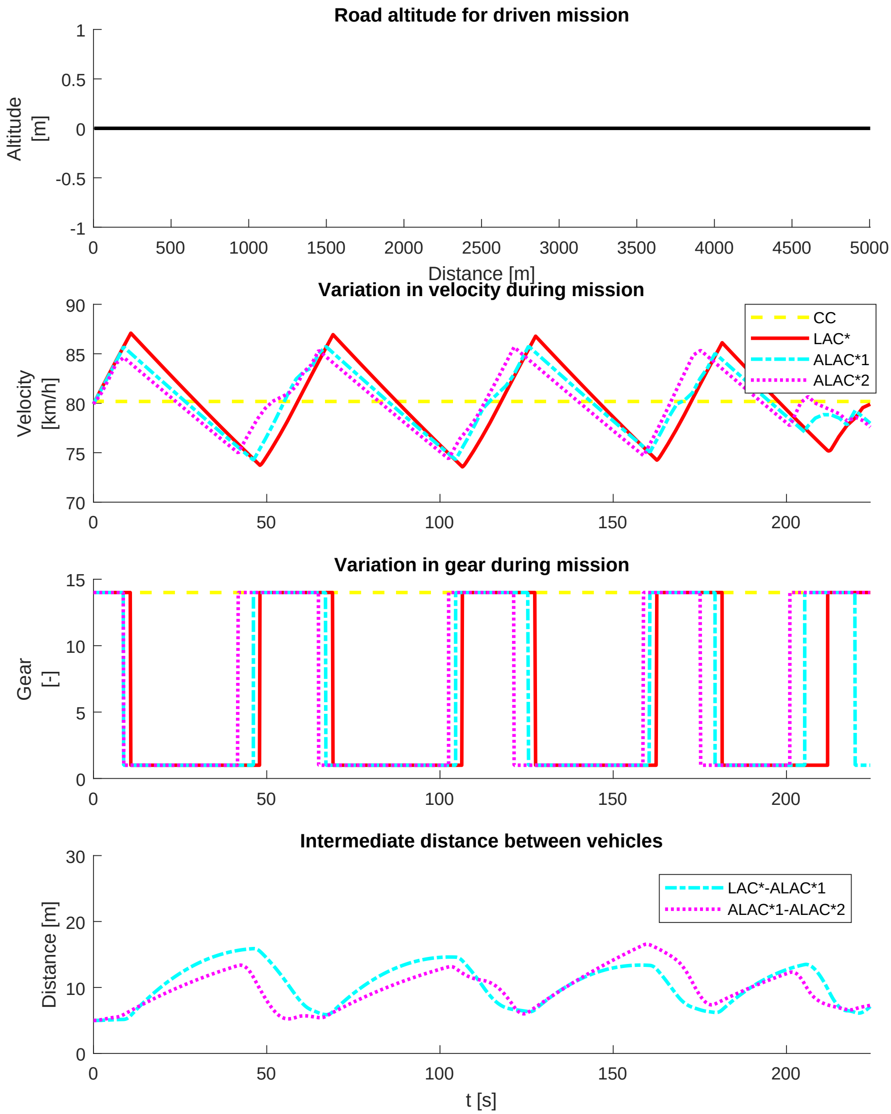

Figure A.2: *Velocity, intermediate distance and gear profiles when simulating 3 vehicles on a flat road. PnG is allowed.*

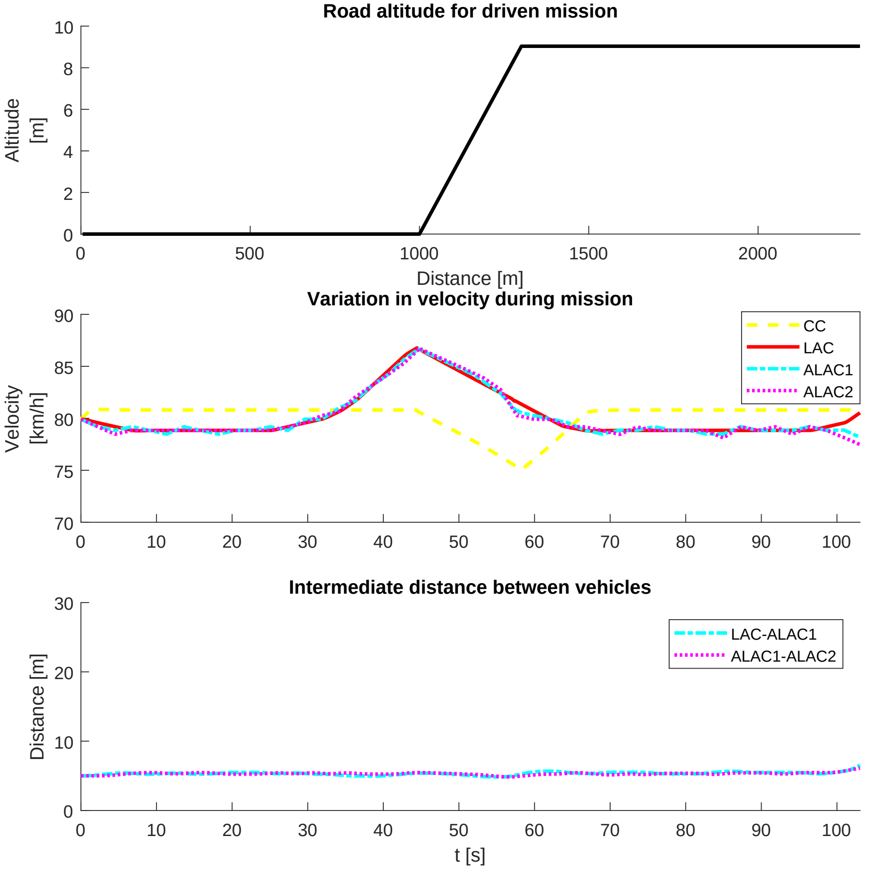

Figure A.3: *Velocity and intermediate distance profiles when simulating 3 vehicles driving uphill. PnG is not allowed.*

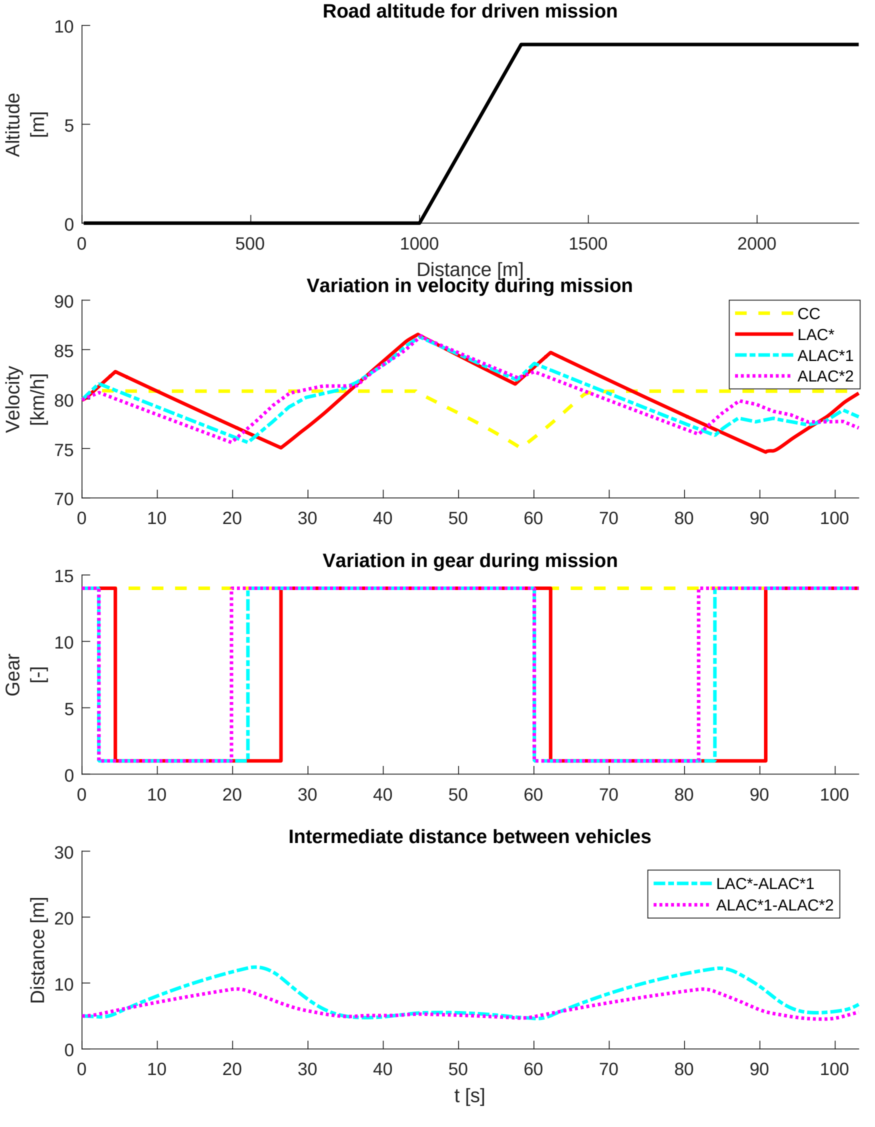

Figure A.4: *Velocity, intermediate distance and gear profiles when simulating 3 vehicles driving uphill. PnG is allowed.*

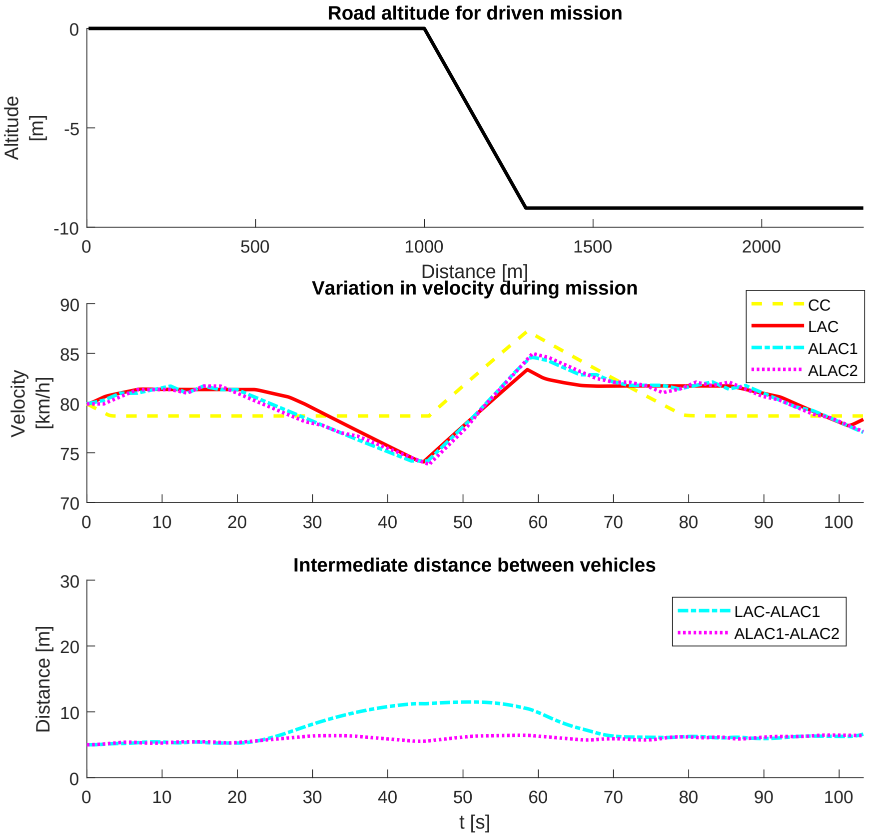

Figure A.5: *Velocity and intermediate distance profiles when simulating 3 vehicles driving downhill. PnG is not allowed.*

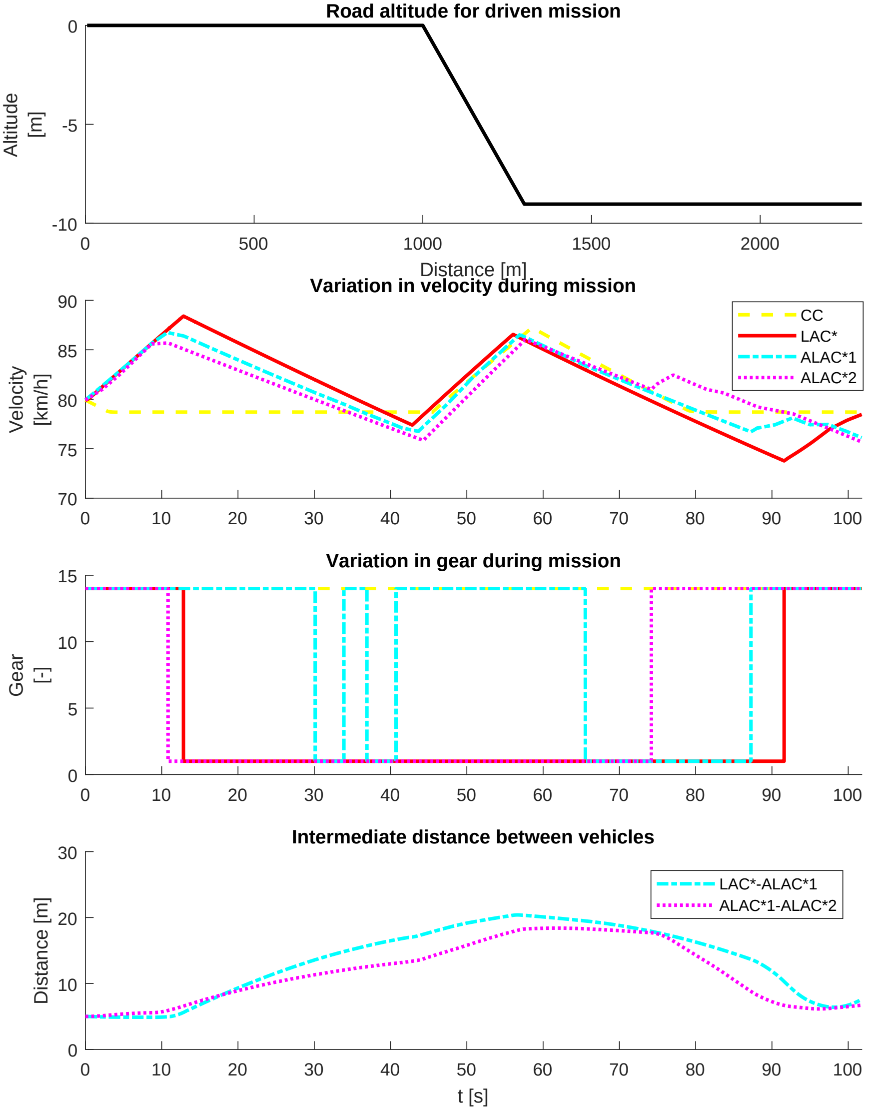

Figure A.6: *Velocity, intermediate distance and gear profiles when simulating 3 vehicles driving uphill. PnG is allowed.*

Bibliography

[1] Scania CV AB. Scania annual report 2010. 2010. Cited on page 1.

[2] Assad Alam. *Fuel-Efficient Heavy-Duty Vehicle Platooning*. PhD thesis, KTH, Royal Institute of Technology, 2014. URL `http://urn.kb.se/resolve?urn=urn:nbn:se:kth:diva-145560`. QC 20140527. Cited on pages 1, 2, 5, 6, 7, 9, 10, 11, and 60.

[3] Daniel Axehill and Johan Sjöberg. Adaptive cruise control for heavy vehicles: Hybrid control and mpc. Master's thesis, Linköping University, Institutionen för systemteknik, 2003. URL `http://urn.kb.se/resolve?urn=urn:nbn:se:liu:diva-1604`. Cited on page 10.

[4] R.E. Bellman. *Dynamic Programming*. Princeton University Press, Princeton, New Jersey, 1957. Cited on page 7.

[5] R.E. Bellman. *Adaptive Control Processes: A Guided Tour*. Princeton University Press, Princeton, New Jersey, 1961. Cited on pages 8 and 25.

[6] Moritz Diehl, Hans Georg Bock, Holger Diedam, and Pierre-Brice Wieber. Fast direct multiple shooting algorithms for optimal robot control. In *Fast Motions in Biomechanics and Robotics, 2005*, Heidelberg, Germany, 2005. Cited on pages 7 and 8.

[7] Kristoffer Ekberg, Viktor Leek, and Lars Eriksson. Optimal control of wastegate throttle and fuel injection for a heavy-duty turbocharged diesel engine during tip-in. In *58th Conference on Simulation and Modelling (SIMS 58)*, Reykjavik, Iceland, 2017. Cited on pages 5, 6, and 16.

[8] Lars Eriksson and Lars Nielsen. *Modeling and Control of Engines and Drivelines*. John Wiley and Sons Ltd, United Kingdom, Chichester, 2014. Cited on pages 1, 6, and 22.

[9] Anders Fröberg, Erik Hellström, and Lars Nielsen. *Explicit Fuel Optimal Speed Profiles for Heavy Trucks on a Set of Topograhic Road Profiles*. 2006. ISBN 978-0-7680-1738-0. URL `http://urn.kb.se/resolve?urn=urn:nbn:se:liu:diva-13146`. Cited on page 33.

[10] Torkel Glad and Lennart Ljung. *Reglerteknik*. Studentlitteratr, Lund, Sweden, 4 edition, 2006. ISBN 978-91-44-02275-8. Cited on page 41.

[11] Lino Guzzella and Antonio Sciarretta. *Vehicle Propulsion Systems, Introduction to Modeling and Optimization*. Springer-Verlag Berlin Heidelberg, New York Dordrecht London, 3 edition, 2013. ISBN 978-3-642-35912-5. Cited on page 16.

[12] Erik Hellström. *Look-ahead Control of Heavy Vehicles*. PhD thesis, Linkoping University, 2010. URL `http://urn.kb.se/resolve?urn=urn:nbn:se:liu:diva-54922`. Cited on pages 1, 2, 5, 7, 8, 15, 26, and 30.

[13] Erik Hellström, Maria Ivarsson, Jan Åslund, and Lars Nielsen. Look-ahead control for heavy trucks to minimize trip time and fuel consumption. *Control Engineering Practice*, 17(2):245–254, 2009. ISSN 1873-6939. doi: 10.1016/j.conengprac.2008.07.005. URL `http://urn.kb.se/resolve?urn=urn:nbn:se:liu:diva-16629`. Cited on page 7.

[14] Erik Hellström, Jan Åslund, and Lars Nielsen. Design of an efficient algorithm for fuel-optimal look-ahead control. *Control Engineering Practice*, 18 (11):1318–1327, 2010. ISSN 1873-6939. doi: 10.1016/j.conengprac.2009.12.008. URL `http://urn.kb.se/resolve?urn=urn:nbn:se:liu:diva-54917`. Cited on page 8.

[15] W. Huang, D.M. Bevly, S. Schnick, and X. Li. Using 3d road geometry to optimize heavy truck fuel efficiency. In *11th International IEEE Conference on Intelligent Transportation Systems*, pages 334–339, 2008. Cited on page 7.

[16] ICCT-Europe. *European vehicle market statistics 2015/16*. Printed pocketbook, 2010. Cited on page 1.

[17] David J. Chang and Edward K. Morlok. Vehicle speed profiles to minimize work and fuel consumption. 131, 03 2005. Cited on page 32.

[18] Josefin Kemppainen. Model predictive control for heavy duty vehicle platooning. Master's thesis, Linkoping University, 2012. Cited on page 21.

[19] F. Lattemann, K. Neiss, S. Terwen, and T. Connolly. The predictive cruise control - a system to reduce fuel consumption of heavy duty trucks. In *SAE World Congress*, number 2014-01-2616 in SAE Technical Paper Series, Detroit, MI, USA, 2004. Cited on page 7.

[20] Gustav Ling and Klas Lindsten. Model predictive control using neural networks: a study on platooning without intervehicular communications. Master's thesis, Linkoping University, 2017. URL `http://urn.kb.se/resolve?urn=urn:nbn:se:liu:diva-139353`. Cited on page 10.

[21] Kevin McDonough, Ilya Kolmanovsky, Dimitar Filev, Diana Yanakiev, Steve Szwabowski, and John Michelini. Stochastic dynamic programming control policies for fuel efficient vehicle following. In *Proceedings of American Control Conference*, Wasthington DC, USA, 2013. Cited on page 9.

[22] Kevin K. McDonough. *Developments in Stochastic Fuel Efficient Cruise Control and Constrained Control with Applications to Aircraft*. PhD thesis, University of Michigan, 2015. URL `http://hdl.handle.net/2027.42/111399`. Cited on page 9.

[23] V.V Monastyrsky and I.M. Golownykh. Rapid computations of optimal control for vehicles. *Transportation Research*, 27B(3):219–227, 1993. Cited on page 25.

[24] Andreas Myklebust and Lars Eriksson. Road slope analysis and filtering for driveline shuffle simulation*. *IFAC Proceedings Volumes*, 45(30):176 – 183, 2012. ISSN 1474-6670. 3rd IFAC Workshop on Engine and Powertrain Control, Simulation and Modeling. Cited on page 6.

[25] Statistical Office of the European Communities. *EUROSTAT: Energy, transport and environment indicators*. Publications Office of the European Union, Luxembourg, Eurostat, 2016. Cited on page 1.

[26] B. Passenberg, P. Kock, and O. Stursberg. Combined time and fuel optimal driving of trucks based on a hybrid model. In *European Control Conference*, Budapest, Hungary, 2009. Cited on page 7.

[27] Magnus Pettersson and Lars Nielsen. Gear shifting by engine control. *IEEE Transactions on Control Systems Technology*, 8(3):495–507, May 2000. ISSN 1063-6536. doi: 10.1109/87.845880. Cited on page 19.

[28] Rajesh Rajamani. *Vehicle Dynamics and Control*. Springer US, New York Dordrecht London, 2 edition, 2012. ISBN 978-1-4614-1432-2. Cited on pages 10, 23, 24, 39, and 40.

[29] Giorgio Rizzoni, Lino Guzzella, and Bernd Baumann. Unified modeling of hybrid electric vehicle drivetrains. *IEEE/ASME Transactions on Mechatronics*, 4(3):246–257, September 1999. Cited on page 16.

[30] S. Terwen, M. Back, and V. Krebs. Predictive powertrain control for heavy duty trucks. In *4th IFAC Symposium on Advances in Automotive Control*, Salerno, Italy, 2005. Cited on page 7.

[31] V. Turri, B. Besselink, and K. H. Johansson. Cooperative look-ahead control for fuel-efficient and safe heavy-duty vehicle platooning. *IEEE Transactions on Control Systems Technology*, 25(1):12–28, Jan 2017. ISSN 1063-6536. doi: 10.1109/TCST.2016.2542044. Cited on page 11.

[32] Valerio Turri, Oscar Flärdh, Jonas Mårtensson, and Karl H. Johansson. Fuel-optimal look-ahead adaptive cruise control for heavy-duty vehicles. Submitted for conference publication, 2018. Cited on pages 8 and 10.

[33] Hans Jakob Walnum and Morten Simonsen. Does driving behavior matter? an analysis of fuel consumption data from heavy-duty trucks. *Transportation Research Part D: Transport and Environment*, 36:107–120, 2015. Cited on page 8.